

<https://doi.org/10.14379/iodp.proc.370.101.2017>

## Expedition 370 summary<sup>1</sup>



V.B. Heuer, F. Inagaki, Y. Morono, Y. Kubo, L. Maeda, S. Bowden, M. Cramm, S. Henkel, T. Hirose, K. Homola, T. Hoshino, A. Ijiri, H. Imachi, N. Kamiya, M. Kaneko, L. Lagostina, H. Manners, H.-L. McClelland, K. Metcalfe, N. Okutsu, D. Pan, M.J. Raudsepp, J. Sauvage, F. Schubotz, A. Spivack, S. Tonai, T. Treude, M.-Y. Tsang, B. Viehweger, D.T. Wang, E. Whitaker, Y. Yamamoto, and K. Yang<sup>2</sup>

**Keywords:** International Ocean Discovery Program, IODP, *Chikyu*, Expedition 370, Site C0023, Muroto Transect, ODP Leg 190, Leg 131, Site 1174, Site 1173, Site 808, deep biosphere, limits of deep subseafloor life, biotic–abiotic transition, low biomass, microbial communities, mesophiles, thermophiles, hyperthermophiles, biomarker, methanogenesis, sulfate reduction, iron reduction, metabolic rate measurement, protothrust zone, décollement, fluid and gas flow, geosphere–biosphere interactions, super-clean technology, QA/QC, temperature limit of life, heat sterilization, heat flow, geothermal gradient, hydrothermal vent, temperature observatory, ash layers, authigenic mineralization, clay mineralization, biogenic gas, thermogenic gas, kerogen, sulfate–methane transition zone, SMTZ, high-pressure incubation, high-temperature incubation, X-ray computed tomography, CT, advanced piston corer temperature tool, APCT-3, KOACH air filtration system, CORK, perfluorocarbon tracer, PFC, Nankai Trough, Shikoku Basin, Japan, Kochi Core Center

## Abstract

International Ocean Discovery Program (IODP) Expedition 370 explored the limits of the biosphere in the deep subseafloor where temperature exceeds the known temperature maximum of microbial life (~120°C) at the sediment/basement interface ~1.2 km below the seafloor. Site C0023 is located in the protothrust zone in the Nankai Trough off Cape Muroto at a water depth of 4776 m, in the vicinity of Ocean Drilling Program (ODP) Sites 808 and 1174. In 2000, ODP Leg 190 revealed the presence of microbial cells at Site 1174 to a depth of ~600 meters below seafloor (mbsf), which corresponds to an estimated temperature of ~70°C, and reliably identified a single zone of elevated cell concentrations just above the décollement at around 800 mbsf, where temperature presumably reached 90°C; no cell count data was reported for other sediment layers in the 70–120°C range because the detection limit of manual cell counting for low-biomass samples was not low enough. With the establishment of Site C0023, we aimed to detect and investigate the presence or absence of life and biological processes at the biotic–abiotic transition utilizing unprecedented analytical sensitivity and precision. Expedition 370 was the first expedition dedicated to subseafloor microbiology that achieved time-critical processing and

analyses of deep biosphere samples, conducting simultaneous shipboard and shore-based investigations.

Our primary objective during Expedition 370 was to study the relationship between the deep subseafloor biosphere and temperature. We comprehensively studied the controls on biomass, activity, and diversity of microbial communities in a subseafloor environment where temperatures increase from ~2°C at the seafloor to ~120°C and thus likely encompasses the biotic–abiotic transition zone. This included investigating whether the supply of fluids containing thermogenic and/or geogenic nutrient and energy substrates may support subseafloor microbial communities in the Nankai accretionary complex. To address these primary scientific objectives and questions, we penetrated 1180 m and recovered 112 cores of sediment and across the sediment/basalt interface. More than 13,000 samples were collected, and selected samples were transferred to the Kochi Core Center by helicopter for simultaneous microbiological sampling and analysis in laboratories with a super-clean environment. In addition to microbiological measurements, we determined the geochemical, geophysical, and hydrogeological characteristics of the sediment and the underlying basement and installed a 13-thermistor sensor borehole temperature observatory into the borehole at Site C0023.

<sup>1</sup> Heuer, V.B., Inagaki, F., Morono, Y., Kubo, Y., Maeda, L., Bowden, S., Cramm, M., Henkel, S., Hirose, T., Homola, K., Hoshino, T., Ijiri, A., Imachi, H., Kamiya, N., Kaneko, M., Lagostina, L., Manners, H., McClelland, H.-L., Metcalfe, K., Okutsu, N., Pan, D., Raudsepp, M.J., Sauvage, J., Schubotz, F., Spivack, A., Tonai, S., Treude, T., Tsang, M.-Y., Viehweger, B., Wang, D.T., Whitaker, E., Yamamoto, Y., and Yang, K., 2017. Expedition 370 summary. In Heuer, V.B., Inagaki, F., Morono, Y., Kubo, Y., Maeda, L., and the Expedition 370 Scientists, *Temperature Limit of the Deep Biosphere off Muroto*. Proceedings of the International Ocean Discovery Program, 370: College Station, TX (International Ocean Discovery Program).

<https://doi.org/10.14379/iodp.proc.370.101.2017>

<sup>2</sup> Expedition 370 Scientists' addresses.

MS 370-101: Published 23 November 2017

This work is distributed under the [Creative Commons Attribution 4.0 International \(CC BY 4.0\) license](#).

## Contents

- [1 Abstract](#)
- [2 Introduction](#)
- [4 Background](#)
- [7 Scientific objectives and hypotheses](#)
- [8 Site C0023 summary](#)
- [16 Accomplishments and future prospectus](#)
- [16 References](#)

## Introduction

Over the course of nearly 50 years of scientific ocean drilling, microbial cells have been found everywhere, even in sediments of Cretaceous age (Roussel et al., 2008), in extremely nutrient poor sediment below the ocean gyres (D'Hondt et al., 2009, 2015; Røy et al., 2012), in the deepest sampled coal-bearing sediments (~2500 meters below seafloor [mbsf]) (Inagaki et al., 2015; Glombitza et al., 2016; Liu et al., 2017), and in basement rocks (Orcutt et al., 2011; Lever et al., 2013). Metabolic rates of deep subseafloor microbes are extraordinarily low (D'Hondt et al., 2002, 2004), with most deeply buried microbial cells physiologically active (Morono et al., 2011; Imachi et al., 2011; Inagaki et al., 2015) or quiescent as dormant phase or spore (Lomstein et al., 2012; Langerhuus et al., 2012). Presumably, the subseafloor contains as many microbial cells as all the water in the global oceans; however, the exact size of the subseafloor biosphere is still a matter of debate (Parkes et al., 1994, 2000; Whitman et al., 1998; Lipp et al., 2008; Kallmeyer et al., 2012; Hinrichs and Inagaki, 2012). To date, the bottom of the deep subseafloor biosphere has not been located, the biosphere–geosphere interactions at this important boundary have not been explored, and it remains to be resolved what poses the ultimate limits to life in the subseafloor. By addressing these scientific challenges, the International Ocean Discovery Program (IODP) aims to shed light on one of the largest continuous ecosystems on Earth (IODP Science Plan, Challenge 6; <http://www.iodp.org/about-iodp/iodp-science-plan-2013-2023>).

Several Integrated Ocean Drilling Program expeditions addressed environmental conditions that potentially limit life in the subseafloor: temperature, pH, salinity, availability of potential metabolic energy and nutrients, fluid flow, and pore space. For example, Integrated Ocean Drilling Program Expedition 329 studied the influence of energy limitation on subseafloor microbial communities in the South Pacific Gyre, where very low concentrations of sedimentary organic matter and its refractory nature strongly limit microbial life and result in aerobic subseafloor sedimentary ecosystems with low cell densities of  $10^3$ – $10^4$  cells/cm $^3$  throughout the sediment column (D'Hondt, Inagaki, Alvarez Zarikian, and the Expedition 329 Scientists, 2011; D'Hondt et al., 2015). Integrated Ocean Drilling Program Expeditions 317 (Canterbury Basin) and 337 (Shimokita Coalbed Biosphere) studied microbial communities in extremely deep sediment (2000 and 2500 mbsf, respectively) (Ciobanu et al., 2014; Inagaki et al., 2015). Although both expeditions presented strong evidence for the presence of microbial life throughout the cored sedimentary sequences, Expedition 337 documented an abrupt decrease in microbial cell concentration deeper than ~1500 mbsf, to levels that are drastically lower than predicted by extrapolation of the global regression line (Inagaki et al., 2015; cf. Parkes et al., 2000, 2014). In spite of the great depths, in situ temperatures did not exceed 60°C.

Temperature is commonly used as the variable that defines the bottom boundary of the deep biosphere in estimates of its size (Whitman et al., 1998; Parkes et al., 2000; Lipp et al., 2008; Heberling et al., 2010; Kallmeyer et al., 2012; Parkes et al., 2014). The currently known upper temperature limit of life for microorganisms inhabiting comparatively energy rich hydrothermal vent environments is at around 120°C (Blöchl et al., 1997; Kashefi and Lovley, 2003; Takai et al., 2008). However, studies of petroleum biodegradation in deeply buried basins suggest that sterilization takes place between 80° and 90°C (Head et al., 2003; Wilhelms et al., 2001), and this finding might be more relevant to the energy-limited deep sub-

seafloor biosphere. The lower temperature limit in subsurface settings relative to hydrothermal settings is possibly linked to the enhanced requirement of metabolic energy at elevated temperatures for the repair of degraded biomolecules (cf. Head et al., 2003; Hoehler and Jørgensen, 2013; Lever et al., 2015); the potential supply of metabolic energy is low in sedimentary settings that tend to be lean in electron acceptors and/or donors compared to hydrothermal vents, at which reduced fluids are mixed with oxygenated seawater. Experimental studies with surface sediment demonstrated a nonlinear effect of temperature on biogeochemistry and prokaryotes, with rapid changes occurring over small temperature intervals, and revealed that substrate addition and increase of metabolic energy result in stimulation of microbial activities at elevated temperatures (Roussel et al., 2015). The influence of temperature on microbial communities was one of the central questions during Integrated Ocean Drilling Program Expedition 331 at the Iheya North hydrothermal field in the Okinawa Trough, but this task was severely complicated by extremely high geothermal gradients. Consequently, microbial life seemed to cease within a few tens of meters below the seafloor, and the strongly condensed temperature zones prevented in-depth examination of critical depth intervals (Takai, Mottl, Nielsen, and the Expedition 331 Scientists, 2011; Yanagawa et al., 2014, 2016).

With the goal of studying the influence of temperature on the amount, activity, and taxonomic composition of deep subseafloor sedimentary communities, IODP Expedition 370 revisited an already well-characterized geological setting with relatively high heat flow: the Muroto Transect in the Nankai Trough off Japan. Expedition 370 established Site C0023 in the vicinity of Ocean Drilling Program (ODP) Sites 1173, 1174, and 808 (Moore et al., 1991; Moore, Taira, Klaus, et al., 2001) about 125 km offshore Kochi Prefecture, 180 km from Cape Muroto, Japan (Figure F1). In this area, the high heat flow results in temperatures of ~110°–130°C at the sediment/basement interface (Moore et al., 1991; Moore and Saffer, 2001). This particular geological setting enables in-depth examination of the putative temperature-dependent biotic–abiotic transition zone with high-temperature resolution: the increase of temperature with depth is still gradual enough for the establishment of distinct depth horizons with suitable conditions for psychrophilic (optimal growth temperature range <20°C), mesophilic (20°–43°C), thermophilic (43°–80°C), and hyperthermophilic (>80°C) microorganisms.

The data sets resulting from ODP Legs 131, 190, and 196 and lessons learned from previous drilling operations guided the scientific and operational approach of Expedition 370. During Leg 190 in 2000, depth profiles of microbial cell concentrations were obtained for Site 1174 by manual microscopic cell counting on the R/V *JOIDES Resolution*. Because this method had a detection limit of  $\sim 10^5$  cells/cm $^3$ , cell concentrations appeared to reach nondetectable levels at sediment depths around 600 mbsf, where estimated in situ temperatures exceed ~70°C (Figure F2) (Shipboard Scientific Party, 2001a). During Expedition 370, we aimed to closely examine the presence of low-biomass microbial communities in the deep and hot sedimentary environment.

Since Leg 190, major advances in cell separation and enumeration technologies for sediment core samples have lowered the minimum quantification limit (MQL) by a factor of ~10,000 (e.g., Kallmeyer, 2011; Morono et al., 2009, 2013, 2014; Morono and Inagaki, 2010). Likewise, the new capacities offered in the “omics” era for elucidation of taxonomic composition (e.g., Inagaki et al., 2006; Sogin et al., 2006), metabolic activity, and function at single-cell to

Figure F1. Map showing heat flow data and ODP/Integrated Ocean Drilling Program transects and sites in the Nankai Trough (modified from Harris et al., 2013). Marine probes (circles), boreholes (stars), and bottom-simulating reflectors (small circles) are color coded by heat flow. On land, circles show borehole values of heat flow.

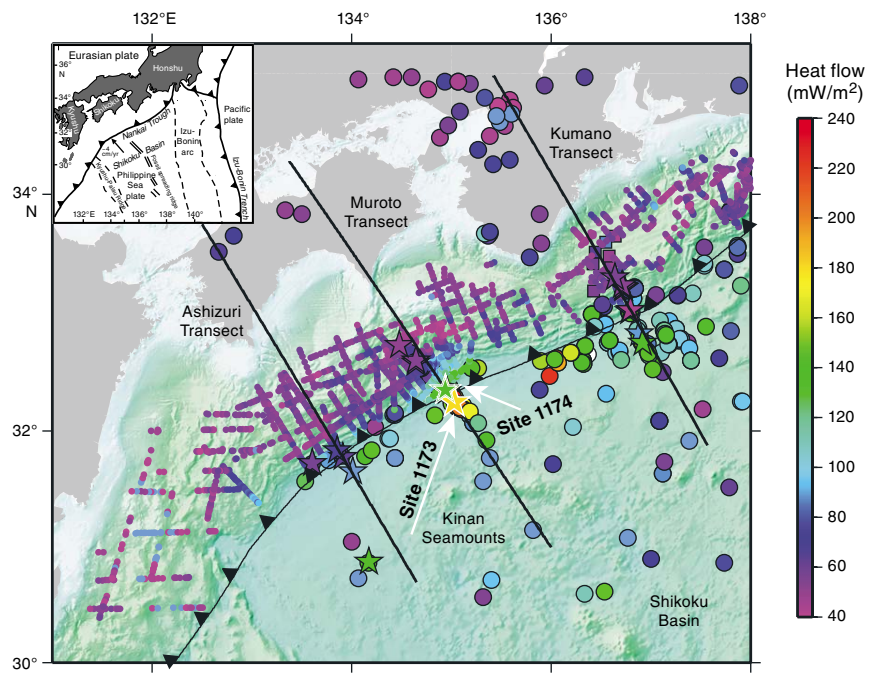
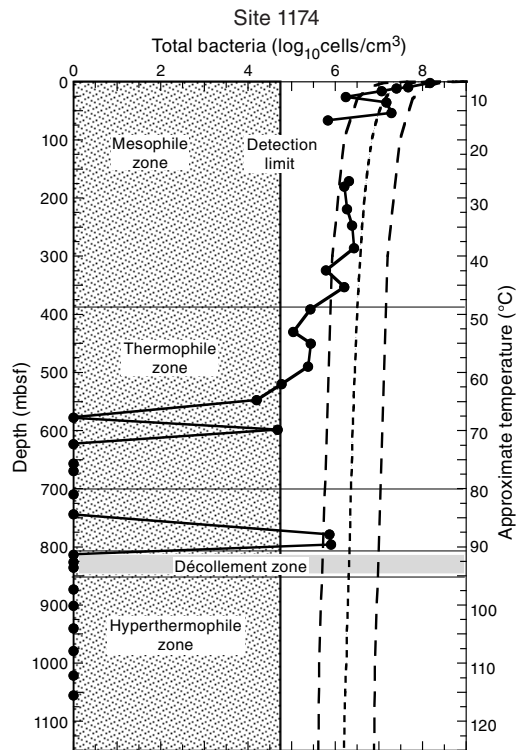


Figure F2. Cell count plots for Site 1174 with depth and temperature axes (Shipboard Scientific Party, 2001c). First drop of cell counts below detection limit occurs around 550 mbsf, which corresponds to  $\sim 65^\circ\text{C}$ . Interestingly, counts exceeded detection limit again in deeper sediment just above the décollement at around 800 mbsf, where temperatures presumably reached  $90^\circ\text{C}$ ; no cell detection was reported for samples from greater depths.



community levels (e.g., Biddle et al., 2008; Lloyd et al., 2013; Orsi et al., 2013), as well as new molecular-isotopic techniques that link biomass to substrate pools (e.g., Biddle et al., 2006; Morono et al., 2011; Wegener et al., 2012) and central metabolic intermediates to distinct geomicrobiological processes (e.g., Heuer et al., 2006, 2009; Zhuang et al., 2014; Wang et al., 2015), allow entirely new approaches to study microbial life close to the limit of the deep biosphere. Recent advances in analytical capabilities provide a tool kit for rigorously examining the unique geosphere–biosphere interactions in geothermally heated sediment that involve the release of microbially utilizable substrates by thermal decomposition of refractory kerogens that otherwise appear resistant to microbial consumption. Thermodynamic modeling can then reveal the actual amounts of energy available and necessary to maintain microbial metabolism (e.g., Hoehler, 2004; Wang et al., 2010; Bethke et al., 2011). The advancement of scientific technologies over the past 15 years has already been shown in part by Expedition 337, which revealed the presence of indigenous microbial cells with concentrations ranging from  $<10^4$  cells/cm $^3$  down to  $\sim 2500$  mbsf in the northwestern Pacific off the Shimokita Peninsula, Japan (Inagaki et al., 2015).

Driven by the recent technological progress in the deep biosphere exploration, Expedition 370 aimed to

- Understand the factors that control biomass, activity, and diversity of microbial communities in a subseafloor environment where temperatures increase from  $\sim 2^\circ\text{C}$  at the sediment/water interface to  $\sim 110^\circ\text{--}130^\circ\text{C}$  at the sediment/basement interface and thus likely encompasses the biotic–abiotic transition zone and
- Determine geochemical, geophysical, and hydrogeological characteristics in sediments and the underlying basaltic basement

and determine if the supply of fluids containing thermogenic and/or geogenic nutrient and energy substrates may support subseafloor microbial communities in the Nankai accretionary complex.

Previous drilling operations have shown that it is challenging to penetrate the geological formation along the Muroto Transect. Therefore, Expedition 370 employed a conservative drilling approach that allowed for the installation of multiple casings in order to create stable hole conditions for reaching the basement and establishing a long-term temperature observatory.

The operational plan was guided by three major objectives:

1. Recovery of high-quality cores from critical temperature intervals of the sedimentary sequence accompanied by monitoring of drilling-induced contamination and quality assurance/quality control (QA/QC) during laboratory procedures. High sample quality and careful contamination controls are prerequisites for investigating the presence (or absence) of life at the lower boundary of the subseafloor biosphere.

2. Recovery of basement core samples to investigate heat and fluid flow in the subducting oceanic crust and thus the potential introduction of basement-derived microbes, nutrients, and electron donors/acceptors into the overlying sediment column.

3. Precise and accurate measurement of in situ temperatures.

Temperature information is essential not only for delineating the impact of temperature on subseafloor life but also for characterizing the heat and fluid flow regime within the Nankai Trough subduction zone. Therefore, in situ temperatures were determined by downhole measurements during drilling as well as by completion of the borehole as an observatory and deployment of thermistor arrays, which will record temperatures in critical temperature intervals for an extended time.

The precise determination of the temperature limit of the deep subseafloor biosphere requires the highest possible sensitivity for the detection of microbial life. In order to fully exploit the technological potential available to date, the scientific work program on board the D/V *Chikyu* was complemented by simultaneous work at the Kochi Core Center (KCC), which is located within reach of a helicopter shuttle for transportation of freshly cored samples. The investigation of microbial communities and processes close to the limits of the subseafloor biosphere benefited in particular from super-clean facilities, aseptic core sampling techniques, and the state-of-the-art analytical infrastructure at KCC. Scientists on board the *Chikyu* and at KCC processed samples, shared data, and reported results together as one “IODP Expedition 370 Scientists” team, according to IODP policies.

## Background

### Geological setting

Located east of Japan between the Shikoku Basin and the Southwest Japan arc, the Nankai Trough marks the subduction boundary between the young, hot Philippine Sea plate and the Eurasian plate (Figure F1). Subduction of the Shikoku Basin occurs at a current rate of ~2–4 cm/y (Seno et al., 1993). With a maximum water depth of 4900 m, the Nankai Trough is relatively shallow, mainly because a thick sediment pile consisting of turbidite layers on top of hemipelagic basin sediment accumulated on the young (~16 Ma) basaltic basement (Taira, Hill, Firth, et al., 1991; Moore, Taira, Klaus, et al.,

2001; Mikada, Becker, Moore, Klaus, et al., 2002). Because of the high flux of terrigenous sediment from the arc to the trench, the Nankai Trough has formed a thick, clastic-dominated accretionary prism over the last ~5 My (Shipboard Scientific Party, 2001a). As the accreted materials are lithified by physical and geochemical processes, the prism accumulates strain energy that is eventually released by seismic activity with a frequency of about one great earthquake every ~180 years during historic times (Ando, 1975).

The Nankai Trough has been investigated intensively throughout the history of scientific ocean drilling. Deep Sea Drilling Project Legs 31 and 87 drilled off Cape Ashizuri to better understand initial mountain building processes (Figure F1) (Shipboard Scientific Party, 1975a, 1975b; Coulbourn, 1986). Legs 131, 190, and 196 continued these studies with a stronger emphasis on the role of dewatering and fluid flow in the consolidation and deformation of sediment off Cape Muroto where the fault and décollement zone at <1000 mbsf are within reach of riserless drilling technology. Six sites were established along the Muroto Transect (Figure F1), covering undeformed to highly deformed zones of the accretionary prism (Taira, Hill, Firth, et al., 1991; Moore, Taira, Klaus, et al., 2001; Mikada, Becker, Moore, Klaus, et al., 2002). During the past decade, the Nankai Trough Seismogenic Zone Experiment (NanTroSEIZE) has investigated this subduction zone with a multidisciplinary and multiphase drilling, sampling, and monitoring program to better understand the plate boundary fault system that has historically produced gigantic earthquakes and tsunamis. About 200 km north of the Muroto Transect, NanTroSEIZE established 13 drilling sites along the Kumano Transect off the Kii Peninsula where the plate boundary fault system is within reach of the *Chikyu*’s riser drilling technology. In the course of numerous seismic and bathymetric surveys, the structure of the Nankai Trough off Shikoku was imaged extensively (e.g., Aoki et al., 1982; Ashi and Taira, 1992; Costa Pisani et al., 2005; Karig, 1986; Kodaira et al., 2000; Le Pichon et al., 1987; Moore et al., 1990, 1991; Okino and Kato, 1995; Park et al., 1999, 2000; Stoffa et al., 1992; Taira and Ashi, 1993). A large volume of 3-D seismic reflection data was acquired in 1999 (R/V *Ewing* Cruise 9907/8) in an effort to image the décollement from the trench into the seismogenic zone (e.g., Bangs et al., 1999, 2004; Bangs and Gulick, 2005; Gulick et al., 2004).

For elucidating the temperature limit of the deep subseafloor biosphere, the Muroto Transect is more suitable than the Kumano Transect, as the deeply buried sediment is exposed to higher temperatures. Expedition 370 established Site C0023 in the vicinity of Sites 808 and 1174 (Figures F3, F4) in the protothrust zone of the accretionary prism (Figure F5), where ~16 Ma basaltic basement is covered with the following series of sediment types (Figure F6): volcaniclastic facies, lower Shikoku Basin facies (hemipelagic mudstone), upper Shikoku Basin facies (hemipelagic mudstone with abundant volcanic ash layers), basin-to-trench transition, and outer and axial trench wedge facies, on top of which, finally, slope apron facies have been deposited (Shipboard Scientific Party, 2001b, 2001c). Site 1174 subsided at a moderate rate of ~50 m/My during the Miocene and the Pliocene, before rates changed dramatically in the Quaternary. The rate of subsidence rose 12-fold to ~600 m/My and resulted in a high heating rate of up to 130 K/My (Horsfield et al., 2006). Deformation bands have developed deeper than 218 mbsf, and at 808–840 mbsf a distinct 32 m thick décollement zone separates the protothrust domain with fractured and steepened bedding (<807.6 mbsf) from a relatively little deformed underthrust section (>840.2 mbsf) (Shipboard Scientific Party, 2001c).

Figure F3. Regional bathymetry map around Site C0023. Locations of Site C0023 (yellow) and existing nearby ODP drill sites (white) are shown. Black box = area of 3-D seismic reflection volume along Muroto Transect (Bangs et al., 2004; Gulick et al., 2004; Moore, Taira, Klaus, et al., 2001). Inset: general tectonic configuration of Japanese Island system.

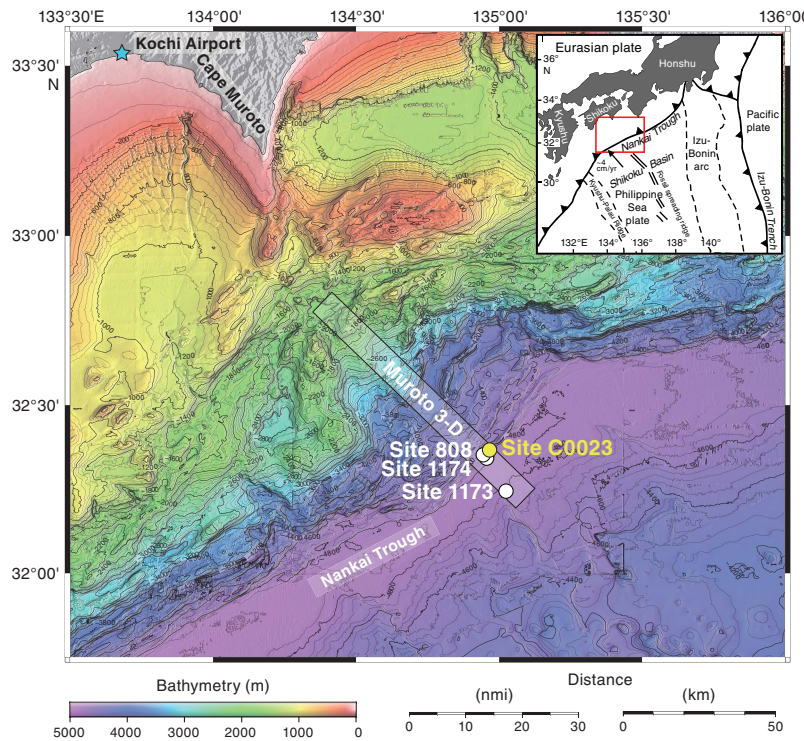


Figure F4. Close-up bathymetry map around Site C0023. Yellow circle = Site C0023, white circles = existing nearby ODP drill sites. Red outline = area of 3-D seismic reflection volume of Muroto Transect, yellow dashed lines = cropped seismic sections of In-line (IL) 332 and Cross-line (XL) 781. MCS = multichannel seismic.

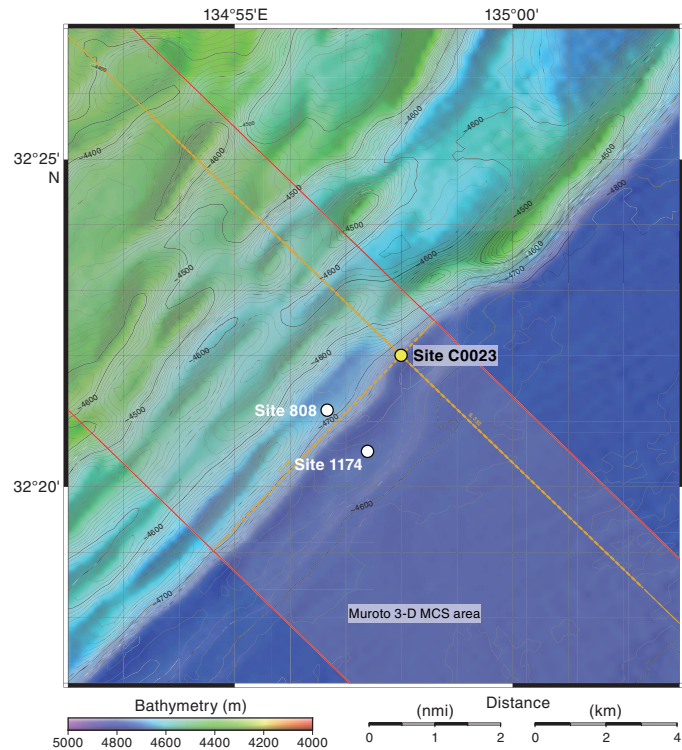


Figure F5. Prestack depth migration seismic section of IL 332 cropped into region of interest. Original data are available at <http://www-udc.ig.utexas.edu/sdc/cruise.php?cruiseID=ew9907>. Blue line = position of Site C0023 (with a depth scale in meters below seafloor), green arrows = horizons of top of décollement zone and oceanic basement. MSL = from mean sea level.

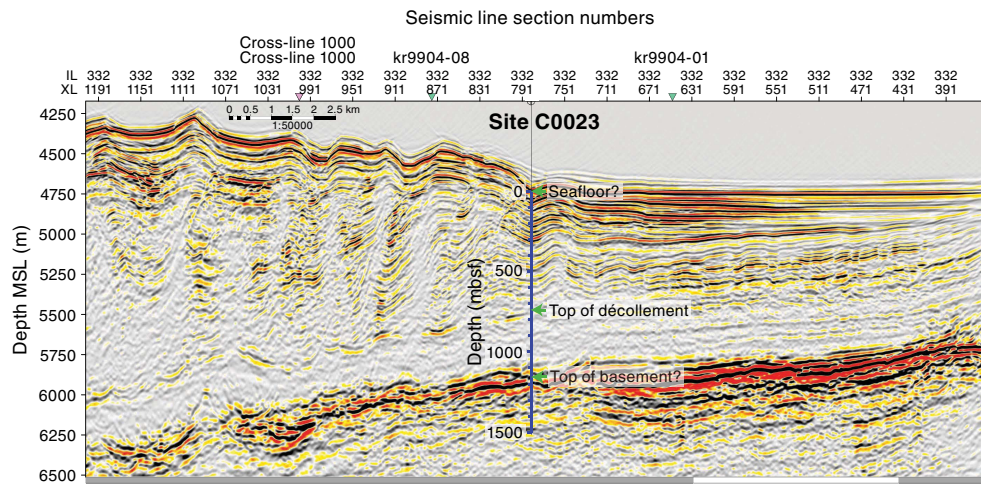
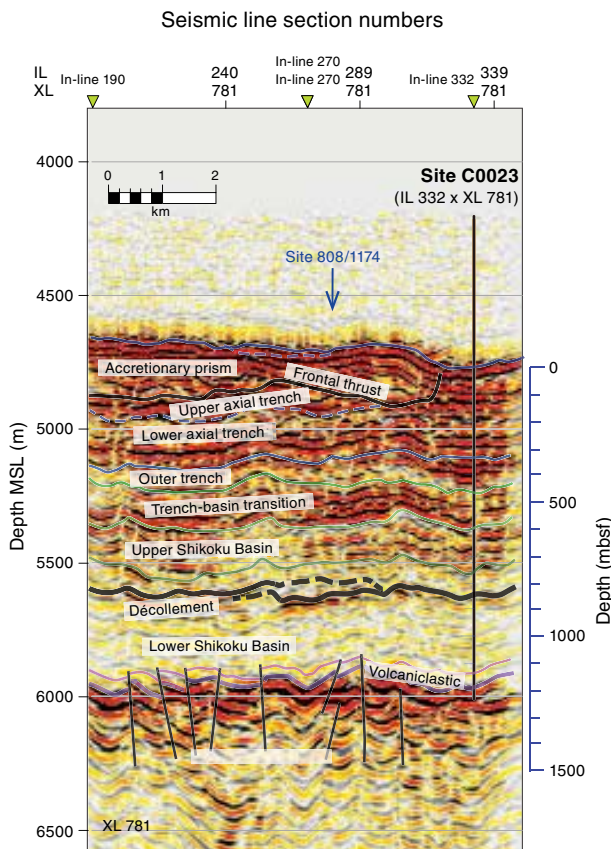


Figure F6. Depth-converted prestack time migration seismic section of IL 781 cropped into region of interest with geological interpretation. Original data are available at <http://www-udc.ig.utexas.edu/sdc/cruise.php?cruiseID=ew9907>. Blue arrow = projected position of Sites 808 and 1174.



## Heat and fluid flow

There is compelling evidence for hydrothermal circulation in the subducting oceanic crust, which leads to elevated heat flux at the deformation front (Figure F1). Specifically, thermal and geochemical models suggest that advective heat and fluid flow in the subducting oceanic crust are crucial for extracting and redistributing heat (Harris et al., 2013; Spinelli and Wang, 2008), whereas the accreted sediment expels fluids mainly by upward diffusive flow through a large portion of the accretionary prism (Taira, Hill, Firth, et al., 1991; Taira et al., 1992). Pore water profiles did not clearly indicate active fluid flow along the décollement or along the frontal thrust, and fractures within the décollement zone were found to be not mineralized (Taira, Hill, Firth, et al., 1991; Maltman et al., 1992; Moore, Taira, Klaus, et al., 2001); however, at >400–500 mbsf, pore water freshening is detectable in Cl<sup>-</sup> concentrations that are lower than seawater values (cf. Kastner et al., 1993). The observed freshening is partly explained by in situ diagenesis (i.e., compaction and thermally driven smectite dehydration) but also suggests some episodic lateral fluid flow along one or more sediment horizons (Moore, Taira, Klaus, et al., 2001; Saffer and Bekins, 1998; Underwood et al., 1993).

Sites 1174 and C0023 are located in a zone of high heat flow that encompasses the trench and the lowermost part of the prism (Figure F1). The surface heat flux consistently exceeds 100 mW/m<sup>2</sup> in this region and amounts to ~180 mW/m<sup>2</sup> at Site 1174 but steeply declines landward of the deformation front to values of ~60 mW/m<sup>2</sup> and scatters largely around 82 mW/m<sup>2</sup> seaward in the Shikoku Basin (Yamano et al., 1984; Kinoshita and Yamano, 1986; Shipboard Scientific Party, 1991, 2001b, 2001c; Spinelli and Underwood, 2005; Harris et al., 2013; Yamano et al., 1992). Based on available heat flow data, the heat flow was expected to be 156 mW/m<sup>2</sup> at Site C0023, and in situ temperatures were estimated to reach ~110°–130°C at the sediment/basement interface (Hinrichs et al., 2016).

## Physical properties

Measurements of physical properties in sediment and basement rock, particularly their variations with depth, are a major target in studies of rock mechanics and fault zone seismogenesis. With increasing temperature and pressure, physicochemical alteration is facilitated, causing lithification and diagenesis of the sediment (Moore and Saffer, 2001). These processes modify the composition of the fault gouge and result in authigenic growth of clay minerals (e.g., Chester et al., 1993; Wintsch et al., 1995), which are known to have profound effects on fault strength and potential instability (e.g., Byerlee and Summers, 1975; Ikari et al., 2009). In particular, the smectite-to-illite reaction, which is typically observed at 60°–150°C (i.e., temperatures typical of the updip seismicity limit [Vrolijk, 1990]), releases fluids and silica into the pore space. Released silica acts as a cementing agent (Towe, 1962; Spinelli et al., 2007) and thus strengthens the frictional properties of the materials (e.g., Mair and Marone, 1999) while lowering their effective porosity (Spinelli et al., 2007). At the same time, the release of mineral-derived water from desorption and clay mineral transformation reactions into an environment in which precipitation has decreased porosity may cause high pore pressure and subsequent hydrofracturing of the rock (Behrmann, 1991). Elevated pressures and temperatures typical of upper seismogenic zones are also known to enhance porosity loss in sediment (Hüpers and Kopf, 2009) and are associated with decreases in permeability. The result is a dense, cemented rock that differs substantially from homogeneous sediment and may thus impose additional limits to the deep subseafloor biosphere.

## Microbiology and geochemistry

Whereas previous investigations focused on the dynamics of deformation and fluid flow processes in the accretionary prism, the abundance of microbial cells in sediment was determined by shipboard cell counting (Figure F2), and the geochemistry of sediment and its interstitial water were characterized as well (Moore, Taira, Klaus, et al., 2001). At Site 1174, cell concentrations were in a range typical for continental margin sediment but decreased to levels below the MQL deeper than ~600 mbsf, where the estimated in situ temperature exceeds ~70°C. Interestingly, cell counts exceeded the MQL again in deeper sediment just above the décollement around 800 mbsf where temperatures reached 90°C; no cell detection was reported at greater depth.

At Site 1174, organic carbon contents ranged from 0.03% to 0.84% and overall decreased with depth (Moore, Taira, Klaus, et al., 2001). In particular, the transition from upper to lower Shikoku Basin facies corresponded to a drop in total organic carbon (TOC) content. Carbon/nitrogen ratios <10 indicated predominantly marine organic matter sources. Pore water sulfate was consumed rapidly in surface sediment and a shallow sulfate–methane transition zone (SMTZ) was found at 3–6 mbsf, but sulfate concentrations increased again throughout the ~490 m thick lower Shikoku Basin sediment and linear concentration gradients were consistent with diffusive flux of sulfate from the oceanic basement into the overlying sediment (Shipboard Scientific Party, 2001b, 2001c; Horsfield et al., 2006). Methane concentrations were highest at 300–660 mbsf (~60°–100°C) and remained relatively high in the presence of sulfate deeper than 660 mbsf (Shipboard Scientific Party, 2001c). Ethane concentrations increased with depth and pointed to thermogenic sources deeper than 900 mbsf (Shipboard Scientific Party, 2001b, 2001c; Horsfield et al., 2006). These observations agree well with findings at adjacent Site 808, where the stable carbon and hydrogen

isotopic composition of methane points to microbial CO<sub>2</sub> reduction as the major methane source in sediment between 20 and 1000 mbsf and to an increasing contribution of thermogenic methane at greater depth (Berner and Faber, 1993). Results of Rock-Eval pyrolysis revealed significant thermal transformation of organic matter deeper than 500 mbsf, suggesting in situ production of hydrocarbon gases, hydrogen, and oxygenated low-molecular weight compounds (Horsfield et al., 2006). Yet, the interplay of thermogenic and biogenic processes and their relevance for the supply of metabolic energy and substrates remain to be explored.

## Scientific objectives and hypotheses

Expedition 370 was primarily motivated by Challenge 6 in the IODP Science Plan (<http://www.iodp.org/about-iodp/iodp-science-plan-2013-2023>) “What are the limits of life in the subseafloor?” and by Challenge 5 “What are the origin, composition, and global significance of subseafloor communities?”

The overarching scientific objectives of Expedition 370 were as follows.

1. *Study subseafloor sedimentary microbial communities situated in temperature ranges that cover the putative temperature limit of microbial life in anoxic sedimentary systems.*

We aimed to test the hypothesis that temperature increase with depth is accompanied by substantial changes in the composition, function, and activity of microbial communities and that their population density decreases gradually rather than abruptly as suggested by previous examination of Site 1174. Using state-of-the-art microbiological and geochemical techniques, samples obtained during Expedition 370 can provide a far more comprehensive view of the relationship between microbial communities and temperature than was possible during Leg 190.

2. *Characterize the chemical and physical environment in sediment and basement rock at the limit of the deep subseafloor biosphere.*

We aimed to test the hypothesis that the cored sections harbor biotic–abiotic transition zones and that unique geochemical and microbial signatures can be identified within the sediment, rock, and fluid matrixes that differentiate the biotic and abiotic realms and/or their transitions. Samples obtained during Expedition 370 will be investigated in detail with respect to (bio)chemical, isotopic, mineralogical, and physical properties and changes thereof.

3. *Examine the relationship between thermogenic release of potential substrates and microbial life.*

Expedition 370 aimed to obtain samples to test existing hypotheses (Horsfield et al., 2006; Parkes et al., 2007) that predict stimulation of microbial activity by thermal decomposition of organic matter. To that end, we will conduct studies of genes, their expression, cultivation-dependent and -independent assays, biogeochemical activity measurements, and advanced organic geochemical analyses that specifically target potential substrates for microbial life, as well as document structural modifications of macromolecular organic matter induced by their release.

In addition, Expedition 370 retrieved samples to specifically address the following questions:

- Do subseafloor sedimentary microbial communities populate sediments that lie within the temperature range close to the putative limit of microbial life?

- Is the temperature increase with depth accompanied by substantial changes in the composition, function, and activity of microbial communities?
- Does the population density of microbial communities decrease gradually or abruptly with increasing temperature? And do features like porosity or fluid movement and the introduction of electron acceptors influence the location of the limit to life such that it “flickers out” over a certain depth range rather than “blinks out abruptly” at a specific depth? For example, is microbial activity stimulated by fluid flow regimes?
- Are microbial spores abundant in sediment, and do they germinate when temperatures increase with sediment burial?
- Which microorganisms and processes occur in the deep and hot SMTZ?
- What is the virus distribution in sediments? Are there any host-free viruses in the lifeless (i.e., no prokaryotic cells) zone? And what is the functional role of viruses with regard to the genetic evolution of subseafloor microbial ecosystems?

Characterizing the chemical and physical environment in sediment and basement rock at the limit of the deep subseafloor biosphere will allow us to address questions such as

- Which mechanisms guide the selection of microorganisms at elevated temperatures?
- Are there other adaptations evident in cells present at the bottom of the deep biosphere besides tolerance to high temperatures?
- Do pairs of electron acceptors and donors accumulate that would normally be consumed by biologically mediated redox reactions?
- Is there a measurable impact of smectite–illite reaction on subseafloor microbial communities?
- Does the presumed availability of electron acceptor-rich fluids in the basement stimulate microbial activity in the overlying sediment? If there are active (or survived) microbial communities in the high-temperature basaltic habitat, is there evidence for the inoculation of overlying sediment with basement-derived microbes?
- What is the extent and distribution of hydrothermal veining and crustal alteration related to circulation of basement fluids? How much of this alteration may be related to microbial activity? How large are heat and fluid flow in the subducting oceanic crust?

Elucidating the temperature limit of the deep subseafloor biosphere and biogeochemical processes occurring at the biotic–abiotic transition zone(s) require the highest possible sensitivity for the reliable detection of indigenous microbial life. Therefore, QA and QC were key objectives throughout drilling operations and all subsequent sample handling procedures in the laboratory. Moreover precise and accurate information on in situ temperatures is essential not only for delineating the impact of temperature on subseafloor life but also for characterizing the heat and fluid flow regime within the Nankai Trough subduction zone. Therefore, measurements of

formation temperatures in situ and of thermal conductivity of the cored material were crucial objectives of Expedition 370. An initial set of in situ temperature data was obtained by downhole measurements during drilling. In addition, we aimed to prepare the borehole for its future use as a long-term observatory by installing casing, a remotely operated vehicle (ROV) landing platform, and a CORK head, as well as temperature sensors.

## Site C0023 summary

Site C0023 (32°22.00'N, 134°57.98'E; 4776 m water depth) was established on 17 September 2016 in the vicinity of Sites 1174 and 808 (Figure F4). After stabilizing Hole C0023A with a 20 inch drill-in casing to 181 mbsf, 83 cores were taken from 189 to 871 mbsf. A spot-coring approach employing a short advance modified hydraulic piston coring system (short HPCS) equipped with an advanced piston corer temperature tool (APCT-3) for in situ temperature measurements was successfully used for the first time to 410.5 mbsf. Deeper, continuous rotary core barrel (RCB) coring followed. Due to deteriorating borehole conditions, a second casing (13½ inch) was considered necessary on 11 October and installed to 858 mbsf. RCB coring resumed on 25 October and continued until basement was reached on 3 November. Coring terminated with the recovery of Core 370-C0023A-112R from a total drilling depth of 1180 mbsf. Recovery was 75.9% on average and yielded altogether 577.85 m of core (Tables T1, T2). During the expedition, more than 13,000 samples were taken from these cores and preserved for shipboard and shore-based analyses as well as for the postexpedition research of more than 90 individual scientists who requested samples from Site C0023.

To ensure the best sample quality, we employed a multistep procedure to remove the potentially contaminated part of the cores. All samples for time-, oxygen-, and contamination-sensitive microbiological and biogeochemical investigations were taken in the form of whole-round cores (WRCs) from the most undisturbed parts of freshly retrieved core sections, which were identified by careful visual inspection using X-ray computed tomography (CT) image scans. Core intervals with obvious fractures and/or drilling disturbances were strictly avoided, as such structures might provide pathways for the introduction of contamination into the interior of the core. The outer layer of the WRCs was removed immediately after retrieval to avoid potential intrusion of contaminants from drilling fluid. Whole-round sampling was completed as soon as possible, usually within a few hours after a core had arrived on deck. Samples for oxygen-sensitive analyses were processed under anaerobic conditions. For microbiological samples, a super-clean and anaerobic working environment was established by installing a tabletop air filtration unit and ionizer (i.e., static eliminator) inside an anaerobic chamber, preventing potential sample contamination by laboratory air. In order to avoid alteration of samples and loss of information during storage, in-depth investigations were started as soon as possible after core recovery. To this end, the carefully cleaned and anaerobically packed samples were transported to shore by helicopter

Table T1. Expedition 370 hole summary. mbsl = meters below sea level. [Download table in CSV format.](#)

Hole	Latitude	Longitude	Water depth (mbsl)	Cores (N)	Cored interval (m)	Recovered length (m)	Recovery (%)	Drilled interval (m)	Penetration (m)	Time on site (days)
C0023A	32°22.0018'N	134°57.9844'E	4775.5	112	761.7	577.85	75.9	418.3	1180	58

Table T2. Site C0023 core summary. DSF = drilling depth below seafloor. (Continued on next page.) [Download table in CSV format](#).

Core	Core on deck date (2016)	Core on deck time UTC (h)	Top depth drilled DSF (mbsf)	Interval advanced (m)	Recovered length (m)	Core recovery (%)	Comment
370-C0023A-							
1F	20 Sep	0810	189.0	1.5	1.77	118.0	
2F	21 Sep	1629	203.0	1.2	1.20	100.0	
3F	21 Sep	1942	205.0	2.0	3.60	180.0	
4F	22 Sep	0230	253.0	2.0	2.54	127.0	
5F	22 Sep	0940	255.0	2.0	3.70	185.0	
6F	22 Sep	1550	303.0	2.0	1.50	75.0	
7X	22 Sep	1956	305.0	9.5	6.60	69.5	
8F	23 Sep	0412	314.5	2.0	0.77	38.5	
9F	23 Sep	0821	316.5	2.0	3.65	182.5	
10F	23 Sep	1923	353.0	2.0	1.82	91.0	
11F	23 Sep	2213	355.0	2.0	1.21	60.5	
12F	24 Sep	0110	357.0	2.0	1.73	86.5	
13F	24 Sep	0333	359.0	2.0	1.97	98.5	
14X	24 Sep	1242	403.0	4.5	3.50	77.8	
15F	24 Sep	1636	407.5	3.0	0.63	21.0	
16R	27 Sep	0827	410.5	8.0	8.47	105.9	
17R	27 Sep	1216	418.5	9.5	3.28	34.5	
18R	27 Sep	1506	428.0	9.5	8.34	87.8	
19R	27 Sep	1856	437.5	9.5	9.00	94.7	
20R	27 Sep	2211	447.0	9.0	6.34	70.4	
21R	28 Sep	0223	456.0	9.5	6.30	66.3	
22R	28 Sep	0515	465.5	9.5	8.48	89.3	
23R	28 Sep	0823	475.0	9.5	6.45	67.9	
24R	28 Sep	1152	484.5	9.5	10.24	107.8	
25R	28 Sep	1527	494.0	9.5	8.37	88.1	
26R	28 Sep	1847	503.5	9.5	8.45	88.9	
27R	28 Sep	2211	513.0	9.5	2.37	24.9	
28R	29 Sep	0126	522.5	9.5	0.00	0.0	
29R	29 Sep	0734	532.0	4.0	1.90	47.5	
30R	29 Sep	1156	536.0	5.0	3.55	71.0	
31R	29 Sep	1436	541.0	9.5	8.20	86.3	
32R	29 Sep	1820	550.5	9.5	2.82	29.7	
33R	29 Sep	2223	560.0	9.5	10.52	110.7	
34R	30 Sep	0152	569.5	4.0	1.98	49.5	
35R	30 Sep	0518	573.5	9.5	6.76	71.2	
36R	30 Sep	0813	583.0	9.5	9.15	96.3	
37R	30 Sep	1156	592.5	9.5	4.28	45.1	
38R	30 Sep	1558	602.0	9.5	8.05	84.7	
39R	30 Sep	2036	611.5	9.5	5.86	61.7	
40R	1 Oct	0051	621.0	9.5	9.33	98.2	
41R	1 Oct	0405	630.5	9.5	10.26	108.0	
42R	1 Oct	0714	640.0	9.5	6.23	65.6	
43R	1 Oct	1056	649.5	9.5	10.28	108.2	
44R	1 Oct	1444	659.0	9.5	10.41	109.6	
45R	1 Oct	1809	668.5	4.5	3.20	71.1	
46R	1 Oct	2141	673.0	5.0	5.30	106.0	
47R	2 Oct	0140	678.0	5.0	5.93	118.6	
48R	2 Oct	0454	683.0	4.5	4.58	101.8	
49R	2 Oct	0856	687.5	5.0	3.84	76.8	
50R	2 Oct	1206	692.5	5.0	5.48	109.6	
51R	2 Oct	1556	697.5	5.0	4.79	95.8	
52R	2 Oct	1949	702.5	5.0	2.66	53.2	
53R	3 Oct	0344	707.5	5.0	0.70	14.0	
54R	3 Oct	0752	712.5	5.0	1.90	38.0	
55R	6 Oct	0114	717.5	5.0	4.54	90.8	
56R	6 Oct	0519	722.5	5.0	5.75	115.0	
57R	6 Oct	1014	727.5	5.0	3.58	71.6	
58R	6 Oct	1404	732.5	5.0	2.93	58.6	
59R	6 Oct	1823	737.5	5.0	5.23	104.6	
60R	6 Oct	2244	742.5	5.0	3.53	70.6	
61R	7 Oct	0253	747.5	5.0	4.78	95.6	
62R	7 Oct	0708	752.5	5.0	2.85	57.0	
63R	7 Oct	1108	757.5	5.0	2.53	50.6	
64R	7 Oct	1518	762.5	4.0	1.74	43.5	
65R	7 Oct	2024	766.5	5.0	2.90	58.0	
66R	8 Oct	0115	771.5	3.5	3.79	108.3	
67R	8 Oct	0545	775.0	5.0	3.51	70.2	

Table T2 (continued).

Core	Core on deck date (2016)	Core on deck time UTC (h)	Top depth drilled DSF (mbsf)	Interval advanced (m)	Recovered length (m)	Core recovery (%)	Comment
68R	8 Oct	1002	780.0	5.0	1.45	29.0	
69R	8 Oct	1356	785.0	5.0	2.24	44.8	
70R	8 Oct	1801	790.0	3.0	0.28	9.3	
71R	8 Oct	2154	793.0	5.0	3.55	71.0	
72R	9 Oct	0138	798.0	6.0	1.84	30.7	
73R	9 Oct	0527	804.0	5.0	0.22	4.4	
74R	9 Oct	1306	809.0	3.0	0.27	9.0	
75R	9 Oct	1821	812.0	4.0	1.36	34.0	
76R	10 Oct	0257	816.0	4.0	2.61	65.3	
77R	10 Oct	0702	820.0	4.0	2.40	60.0	
78R	10 Oct	1058	824.0	4.0	3.80	95.0	
79R	10 Oct	1520	828.0	5.0	4.53	90.6	
80R	10 Oct	2010	833.0	9.5	9.81	103.3	
81R	11 Oct	1727	842.5	9.5	9.61	101.2	
82R	11 Oct	2223	852.0	9.5	4.20	44.2	
83R	12 Oct	0316	861.5	9.5	5.96	62.7	
84R	26 Oct	0142	871.0	9.5	8.62	90.7	
85R	26 Oct	0533	880.5	9.5	5.05	53.2	
86R	26 Oct	1053	890.0	9.5	3.20	33.7	
87R	26 Oct	1458	899.5	9.5	8.88	93.5	
88R	26 Oct	2012	909.0	9.5	5.59	58.8	
89R	27 Oct	0144	918.5	9.5	10.27	108.1	
90R	27 Oct	0730	928.0	9.5	6.07	63.9	
91R	27 Oct	1304	937.5	9.5	10.47	110.2	
92R	27 Oct	1710	947.0	10.0	6.62	66.2	+0.5 m drilling
93R	27 Oct	2050	957.5	10.0	10.40	104.0	+0.5 m drilling
94R	28 Oct	0045	968.0	10.0	10.70	107.0	+0.5 m drilling
95R	28 Oct	0500	978.5	10.0	6.60	66.0	+0.5 m drilling
96R	28 Oct	1432	989.0	10.0	10.27	102.7	+0.5 m drilling
97R	28 Oct	1815	999.5	10.0	9.71	97.1	+0.5 m drilling
98R	28 Oct	2204	1010.0	10.0	10.43	104.3	+0.5 m drilling
99R	29 Oct	0248	1020.5	10.0	10.23	102.3	
100R	29 Oct	0726	1030.5	10.0	6.15	61.5	
101R	29 Oct	1322	1040.5	10.0	10.32	103.2	
102R	29 Oct	1941	1050.5	10.0	8.84	88.4	
103R	30 Oct	0035	1060.5	10.0	10.23	102.3	
104R	30 Oct	0524	1070.5	10.0	7.96	79.6	
105R	30 Oct	1236	1080.5	10.0	3.62	36.2	
106R	30 Oct	1908	1090.5	8.0	4.65	58.1	
107R	31 Oct	0031	1098.5	9.5	5.72	60.2	
108R	31 Oct	0735	1108.0	10.0	5.03	50.3	
109R	31 Oct	1336	1118.0	3.0	3.00	100.0	
110R	31 Oct	2022	1121.0	8.0	5.89	73.6	
111R	3 Nov	1807	1173.0	3.5	0.85	24.3	
112R	3 Nov	2259	1176.5	3.5	0.45	12.9	

shuttle, where they were processed without delay by the shore-based team of expedition scientists at KCC. A total of 92 boxes with high-priority samples were transferred to shore by helicopter on an almost daily basis. At KCC, precleaned core samples were carefully treated in a timely manner for further removal of potentially contaminated surface at either a dust-free super-clean room that meets International Organization for Standardization (ISO) Class 1 clean room standards, an all air exhaust clean bench, or a tabletop air filtration system-equipped anaerobic chamber with monitoring for airborne particles and microbial cells.

On-site operations were completed on 9 November 2016 with the installation of a borehole observatory for long-term in situ temperature measurements to 863 mbsf. The observatory was equipped with an ROV landing platform and a CORK head and was instrumented with thermistor arrays to 863 mbsf. Thermistors monitor temperature mainly inside the cased borehole at 13 depth horizons (Table T3), and data are recorded continuously by data loggers

mounted in the CORK head. Recovery of the data by ROV is planned for March 2018, using the Japan Agency for Marine-Earth Science and Technology research vessel *Kairei* and the ROV *Kaiko*.

The shore-based research program of Expedition 370 at KCC ended on 23 November 2016. By this time, all samples had been cleaned a second time and prepared for further analyses under super-clean conditions. A first set of analyses was completed on selected samples, including cell counts and taxonomic composition of microbial communities. In addition, incubation experiments under high-pressure and high-temperature conditions were started to investigate potential microbial activity.

From an operational point of view, Expedition 370 was successful overall. We carried out nearly all planned operations, established a robust temperature model based on downhole measurements and thermal conductivity data, and conducted all sampling and scientific analyses with an unprecedented high level of QA/QC, precision, and accuracy. With respect to expedition logistics, the smooth

Table T3. Final sensor positions of the temperature observatory, Hole C0023A. Thirteen sensors were deployed along three cables. [Download table in CSV format.](#)

Thermistor cable	Actual depth (mbsf)
1	299.4
3	736.8
3	755.8
3	774.8
2	784.3
3	793.8
2	803.3
1	812.0
3	812.9
2	822.3
2	841.4
1	859.5
2	860.3

operations for the transfer of cored samples from ship to shore, the close collaboration of shipboard and shore-based expedition scientists, and the successful preparation of Expedition 370 with a short lead time of less than 6 months are worth mentioning. Shipboard results for Site C0023 indicate a heat flow of 140 mW/m<sup>2</sup> and temperature of about 120°C at the sediment/basement interface, corroborating the suitability of the environmental setting for addressing research questions as planned.

Preliminary cell count data suggest that cell concentrations are notably lower than those previously reported at Site 1174 but at the same time point to the presence of intact microbial cells in low abundance to at least 850 mbsf. Therefore, the obtained samples and data provide an excellent basis for extensive microbiological, biogeochemical, geological, and geophysical analyses in postexpedition research projects that will potentially provide new insights into the effects of temperature on biological, geochemical, and geophysical processes in the deep subseafloor at Site C0023. Achieving our expedition objectives will significantly expand our knowledge of the factors that limit subseafloor microbial ecosystems at the biotic–abiotic transition zone and ultimately shed more light on the extent and evolutionary nature of the deep subseafloor biosphere on Earth and, more generally, on the habitability of planets.

Although most expedition goals were met, some remain unfulfilled for now but could still be reached during a future return to Hole C0023A. Although the basaltic basement was reached with Cores 111R and 112R, recovery was insufficient to address all related research questions, mainly due to the time constraint. Because of the challenging geological formation, unstable borehole conditions were a major concern throughout the expedition. This fact led us to the decision to set the thermistor array only 5 m deep into the naked hole below the second casing at 858 mbsf. Finally, although thermistor sensor strings with flatpackers were successfully installed during borehole completion, an additional array of miniature temperature loggers was not properly set in the borehole. The underlying reasons for the unsuccessful installation remain to be clarified as of the writing of this report.

Our study site was selected based on previous observations at Sites 1174 and 808, and Site C0023 was established in the closest possible proximity. We found close similarities as well as distinct differences between the new site and the former. In the following,

we provide principal results according to discipline, followed by a synthesis of currently available information pertaining to our scientific objectives.

## Lithostratigraphy

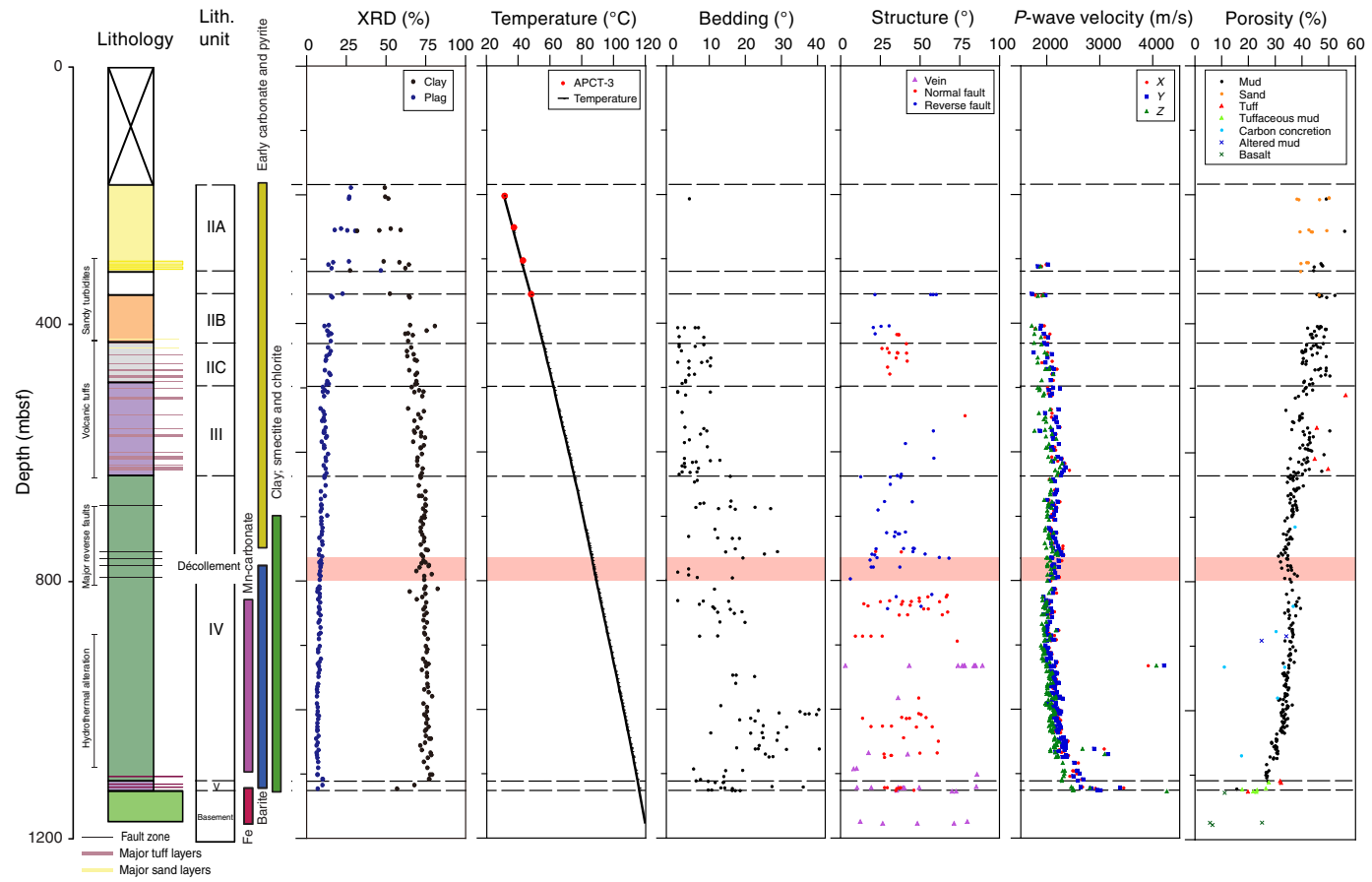
At Site C0023, we recognize four main lithostratigraphic units (Figure F7) that were described before in the lithostratigraphic framework for the Muroto Transect (Taira, Hill, Firth, et al., 1991; Moore, Taira, Klaus, et al., 2001). Near-surface sediment constitutes facies associated with a trench-style deposition. Lithologies include hemipelagic and pelagic mud and mudstone and turbidite-deposited mud, mudstone, silt, and sand. Within this group, we differentiate Subunit IIA (189–318.5 mbsf) that has a higher proportion of sand (axial trench wedge) and Subunit IIB (353–428 mbsf) that has a higher proportion of mud (outer trench wedge facies). We also recognize a third subunit that is transitional between the trench- and volcaniclastic basin-style deposition (Subunit IIC; 428–494 mbsf). This transitional unit evidences some deposition of sand and silt from episodic turbidity currents and some deposition of tuffs and volcaniclastic sediment, also typically from currents. However, mixtures of mud and volcaniclastic sand at Site C0023 only occur because of bioturbation mixing the tops of tuff beds into overlying mud. A solely basin-style deposition is found in Unit III (upper Shikoku Basin facies; 494–637.25 mbsf), and siliciclastic turbidites can no longer be identified. Tuffs and tuffaceous sedimentary rocks constitute <8% of the unit's net thickness but have unique petrophysical and geochemical characteristics that are described later. Unit IV (lower Shikoku Basin facies; 637.25–1112 mbsf) comprises volcanicastics-bearing mudstones that are heavily bioturbated. This latter aspect creates heterogeneity by concentrating ash, shelly bioclasts, and silt, leading to a distinct fabric that creates a template that acts as a focus for strata-bound hydrothermal mineralization. Unit V (acidic volcaniclastic facies; 1112–1125.9 mbsf) is the deepest unit and comprises mudstones and felsic ash, which is less indurated than overlying tuff beds in Subunit IIC and Unit III. A unit of hyaloclastites forms the lithologic basement for Site C0023.

## Structural geology

Bedding planes dip gently, but abrupt changes to steeper dips are observed in the lower Shikoku Basin. Eventually, dip returns back to gentle stratigraphic dips in lithostratigraphic Unit V. Several kinds of deformation structures are distributed at particular depths. Most of the core-scale reverse faults are located above and within the décollement zone (~758–796 mbsf; see **Décollement**, below), whereas dense populations of normal faults were identified beneath the décollement zone (i.e., underthrust sediment). Mineral veins composed of calcite, barite, and anhydrite occur beneath the décollement zone, and most of these are located within or closely associated with faults. Core-scale healed faults that mostly represent a normal fault sense are typically present in the upper Shikoku Basin.

Variations in bedding dip and healed fault distribution at Site C0023 are broadly similar to those at Site 1174. On the other hand, the thicknesses of fault zones within the décollement zone and the nature and distribution of deformation structures in the underthrust sediments at Site C0023 are totally different from Sites 808 and 1174: at Site C0023, the décollement zone is characterized by a thinner fault zone sandwiched between intact mud rock layers, and a dense population of faults and mineral veins is present in the underthrust interval.

Figure F7. Composite figures of lithology, mineralogy, structural geology, and physical properties, Hole C0023A. XRD = X-ray diffraction. Plag = plagioclase.



## Décollement

The onset of the first major fault at 758.15 mbsf was interpreted to mark the top of the décollement zone. Bedding is slightly steepened in the zone (~30°). Below this décollement zone, the fault zone is underlain by generally intact sediment with gentle dips. Although some fault zones were identified in Cores 65R through 71R, most of the recovered cores represent intact surfaces. Therefore, the décollement zone at Site C0023 appears to be composed of alternating intact intervals (approximately several meters in thickness) and thinner fault zones. No thrust fault zone was identified deeper than 796.395 mbsf, and thus this potentially marks the base of the décollement zone.

## Authigenic and hydrothermal mineralization

We recognize five main styles of diagenetic and hydrothermal mineralization at Site C0023. At shallow depths from ~200 to ~700 mbsf, the main authigenic mineralization involves carbonate precipitation and pyritization. This is typically strata bound and can impart significant physical and chemical characteristics to beds (e.g., cementing and causing the early lithification of shallow mudstones or precipitating porosity reducing cements). Clay mineralization occurs from ~700 to ~1000 mbsf and primarily takes the form of smectite and chlorite mineral phases. Such mineralization is typically strata bound and can involve the precipitation of new mineral phases but typically involves the alteration of host lithology. A notable locus for clay mineralization is the décollement zone and

Unit V. Manganese and sulfate mineralization is focused between ~700 and 1100 mbsf. Sulfate mineralization (anhydrite and barite) is heavily associated with veins but is also strata bound and, when sufficiently pervasive, overprints the existing depositional fabric and is also associated with carbonate mineralization. Manganese mineralization is typically strata bound and largely replacive or pore filling and is typically centered on burrows and takes the form of rhodochrosite. Ferrous iron mineralization is found in both Unit V and the lithologic basement. Temperature estimation is hard to constrain at this point, but both the presence of anhydrite and veins of barite and the occurrence of largely stratiform rhodochrosite may indicate temperatures in the 120°–200°C range. Although alteration processes are observed within the décollement zone, overall, they are not of greater magnitude than alteration processes observed at other zones and depths.

## Physical properties

Shipboard physical property measurements, including moisture and density, thermal conductivity, electrical resistivity, *P*-wave velocity, natural gamma radiation, and magnetic susceptibility, were performed on core samples from 204 to 1176 mbsf under room temperature and pressure conditions.

Porosities through the wedge facies (Unit II) to the upper Shikoku Basin facies (Unit III) are characterized by high variability and generally decrease with increasing depth (Figure F7). The lower porosity values represent sand and silty sand at the interval from 200 to 300 mbsf in Subunit IIA, whereas the higher values correlate

with tuff and tuffaceous sediment in Unit III. A high-velocity interval between 620 and 640 mbsf at the base of Unit III corresponds to tuffaceous sediments, although bulk densities of the sediments are lower than surroundings. Within the lower Shikoku Basin facies (Unit IV), porosities continue to decrease with depth to the top of the décollement zone at ~760 mbsf. However, deeper than 760 mbsf, they begin to increase gradually by 5%–7% with depth to ~830 mbsf. This porosity increase is accompanied by a decrease in *P*-wave velocity and apparent formation factor (i.e., electrical resistivity). Deeper than ~830 mbsf, porosities resume a general compaction trend to the base of Unit IV and then rapidly increase within Unit V, where tuffaceous mud becomes the dominant lithology. Basaltic rocks in the basement exhibit a range of porosity between 5.5% and 25%. Similar porosity depth profiles were reported at Sites 808 and 1174 (Taira, Hill, Firth, et al., 1991; Moore, Taira, Klaus, et al., 2001). However, it is a marked contrast at Site C0023 that porosities start increasing gradually within the décollement zone, whereas sharp increase curves in porosity were observed at the base of the décollement zones at Sites 808 and 1174.

In situ temperature measurements between 189 and 408 mbsf and laboratory thermal conductivity measurements indicate a heat flow of 140 mW/m<sup>2</sup>. Assuming that the heat flow is purely conductive and steady state, temperatures of 86° and 120°C are projected for the top of the décollement and the bottom of the hole, respectively (Figure F7).

## Inorganic geochemistry

An extensive suite of interstitial water chemical analyses was performed at Site C0023 to identify potential microbial activity, quantify rates of various metabolic processes, assess the presence of active fluid flow, and complement our understanding of sediment diagenesis in the protolith zone of the Nankai Trough subduction zone off Muroto. High-precision data is required to constrain the geochemical environment, which is fundamental to our understanding of the microbial habitability of the subseafloor.

To fulfill the expedition's principal objectives, we generated high-quality and high-resolution profiles of microbial metabolites

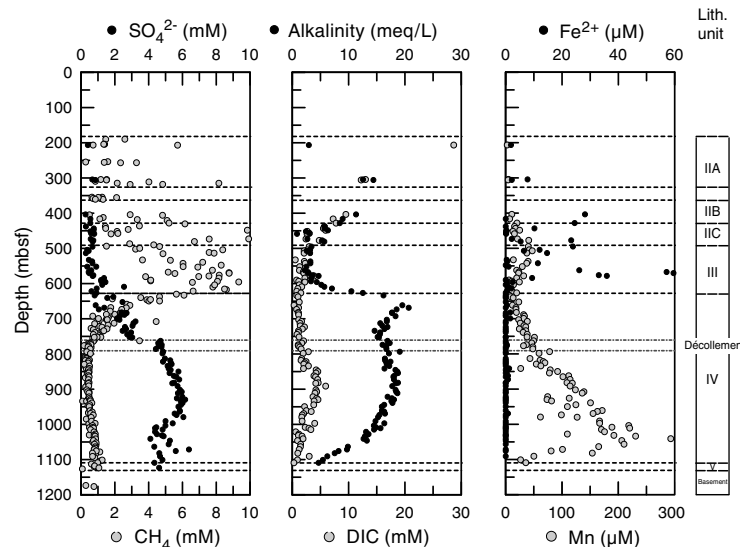
and other elements involved in geochemical processes through high-precision measurement and careful contamination control. The resulting pore water chemistry data set is of unprecedented quality for samples collected with rotary coring technology. The following chemical species were measured on board: chloride, salinity, sulfate, bromide, total alkalinity (TA), dissolved inorganic carbon (DIC), ammonium, sodium, calcium, magnesium, potassium, lithium, boron, barium, aluminum, strontium, manganese, iron, silica, sulfide, hydrogen, and carbon monoxide.

Sulfate in the upper 600 m of the cored formation is assumed to be below detection in situ (measured values are used to determine the extent of contamination of the samples) (Figure F8) and then generally increases with depth. The lower SMTZ at Site C0023 occurs relatively deep (between 630 and 750 mbsf). Complementing the sedimentological identification of the décollement, a sulfate offset of 2.5 mM occurs at 770 mbsf. Starting at 970 mbsf, sulfate sharply decreases by 3 mM to a low-concentration interval within the lowermost 100 m of the formation. The deep sulfate maximum could be relict and/or originate from fluid advection; future work will be required to distinguish between these potential sources.

TA and DIC are similar for the upper 600 m of the cored formation. In contrast to what we would expect if TA was dominated by carbonate alkalinity, TA and DIC diverge at 600 mbsf. TA sharply increases from approximately 4 to 20 mM, peaking at 670 mbsf, whereas DIC remains low and decreases to a minimum of 0.8 mM at 700 mbsf. An offset in DIC (a 3 mM increase) occurs at 850 mbsf. Following the TA peak at 670 mbsf, alkalinity decreases to the décollement before resuming a similar pattern to DIC and smoothly decreasing to the basement. Based on the lack of similarity between DIC and alkalinity profiles in the 600–800 mbsf interval and the detailed analysis of titration curves, we infer that the bulk of the high alkalinity is not derived from the carbonate system but related to the presence of abundant low molecular weight fatty acids.

There are peaks in dissolved Mn and Fe concentrations throughout Units II and III, coinciding with the occurrence of volcanic ash layers. This might indicate the use of Fe and Mn oxyhydroxides as electron acceptors for microbial organic matter

Figure F8. Geochemical profiles for sulfate, methane, alkalinity, DIC, and dissolved ferrous iron and manganese, Hole C0023A. Lithostratigraphic units are also shown.



degradation. As these intervals are considered sulfate- and sulfide-free, dissolution of Fe and Mn oxides due to anaerobic sulfide oxidation seems unlikely. Dissolved sulfide is low (<2  $\mu$ M) in Unit IV, especially around the décollement and at ~930 mbsf. There is no indication for dissolved sulfide in the center of the SMTZ. However, its absence in pore water could potentially be due to a balance between dissolved Fe and sulfide production, which would result in the reaction of these components to solid phase iron sulfides. High manganese concentrations in Unit IV indicate an input by hydrothermal fluids or relict microbial manganese reduction.

### Organic geochemistry

Overall concentrations of calcium carbonate ( $\text{CaCO}_3$ ), TOC, nitrogen, and sulfur at Site C0023 are low in all lithostratigraphic units. The  $\text{CaCO}_3$  profile exhibits a large degree of scatter (ranging from 0.07 to 22 wt%) from 430 mbsf to the basement (1176.6 mbsf), apart from a carbonate-poor interval between 830 and 945 mbsf (middle of Unit IV), in which  $\text{CaCO}_3$  contents are tightly clustered around  $0.61 \pm 0.41$  wt% (mean  $\pm$  standard deviation [SD]). The heterogeneity in the  $\text{CaCO}_3$  data reflects variations in calcite cementation and the presence of calcite veins in the basalt. Low amounts of calcite cementation observed in the carbonate-poor interval are likely responsible for the low  $\text{CaCO}_3$  contents there. TOC monotonically decreases from the top of the cored interval (Subunit IIA, 190 mbsf, 0.5 wt%) to the décollement (~760 mbsf, ~0.2 wt%). Between the décollement and the lower part of Unit IV (1050 mbsf), TOC is roughly constant at  $0.25 \pm 0.04$  wt% before decreasing sharply to minimum values below 0.02 wt% within Unit V. Total nitrogen and sulfur contents are very low throughout Hole C0023A with average values of  $0.05 \pm 0.01$  and  $0.15 \pm 0.11$  wt%, respectively. Low TOC/N ratios of  $5.8 \pm 2.1$  on average are consistent with a predominantly marine source of the organic material.

Dissolved hydrocarbon gases were analyzed from whole-round sections situated adjacent or in close proximity to samples taken for interstitial water analysis. Methane ( $\text{C}_1$ ), ethane ( $\text{C}_2$ ), propane ( $\text{C}_3$ ), *n*-butane ( $n\text{-C}_4$ ), and *i*-butane ( $i\text{-C}_4$ ) were detected within all lithostratigraphic units with varying abundances. Methane concentra-

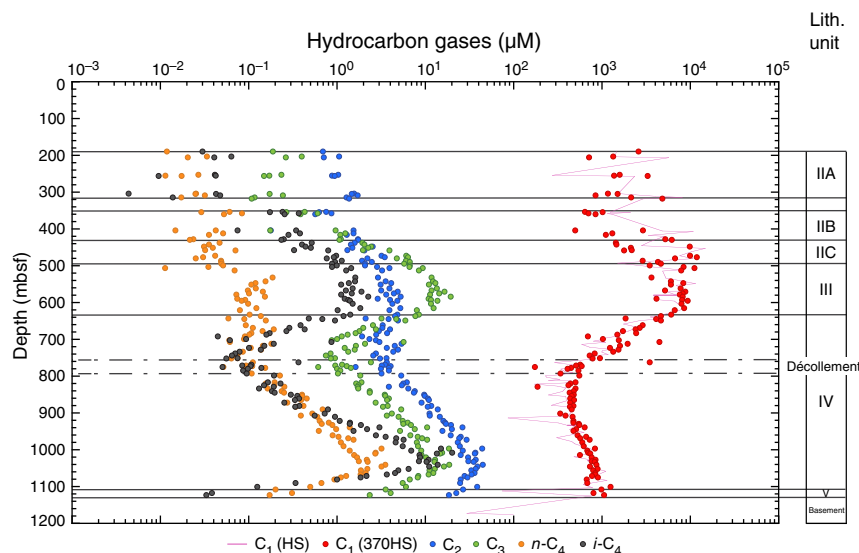
tions show a large scatter in Subunits IIA–IIC, ranging between 0.5 and 11.8 mM and reaching the highest average values of  $7 \pm 2$  mM within Unit III (Figure F9). This apparent peak in methane within Subunit IIC and Unit III coincides with elevated concentrations of propane and *i*-butane relative to the other  $\text{C}_1$ – $\text{C}_4$  hydrocarbons. In this interval, molar concentrations of  $\text{C}_3$  and *i*- $\text{C}_4$  are higher than those of  $\text{C}_2$  and *n*- $\text{C}_4$ , respectively. High molar ratios of methane over ethane ( $\text{C}_1/\text{C}_2 > 10^3$ ) within Subunits IIA–IIC and Unit III are consistent with a dominance of microbially generated methane occurring in these depths. Concentrations of methane decline below Unit III to minimum values of ~0.3 mM within the décollement. This decrease in methane is accompanied by a steady decrease of  $\text{C}_1/\text{C}_2$  to values around  $10^2$  within the décollement. The decline in methane between 660 and 758 mbsf is negatively correlated with concentrations of sulfate, suggesting the presence of an active SMTZ within the upper part of Unit IV above the décollement. The  $\text{C}_{2+}$  hydrocarbon gases also exhibit low concentrations shortly above and within the décollement. Elevated concentrations of  $\text{C}_{2+}$  hydrocarbon gases in the lower part of Unit IV, together with low  $\text{C}_1/\text{C}_2$  ratios, indicate a zone of thermogenic production of these hydrocarbon gases and/or its fluid/gas flow. Below this zone, concentrations of all hydrocarbon gases, except for methane, decrease.

### Microbiology

Minimizing the contamination of potentially extremely low biomass core samples was of highest priority for the microbiological research objectives of Expedition 370. Therefore, rigorous QA/QC efforts and super-clean technologies were implemented, including helicopter transport of freshly taken core samples to the onshore super-clean room facility at KCC. During the expedition, cell counts and DNA-based microbial community fingerprinting were conducted and incubations for probing microbial activity at high-pressure and high-temperature conditions were initiated.

Airborne particle data showed that QC of sample processing and the analytical environment was successful thanks to the use of super-clean technologies. In order to create clean sample handling environments, a tabletop air filtration unit (KOACH T 500-F, Koken

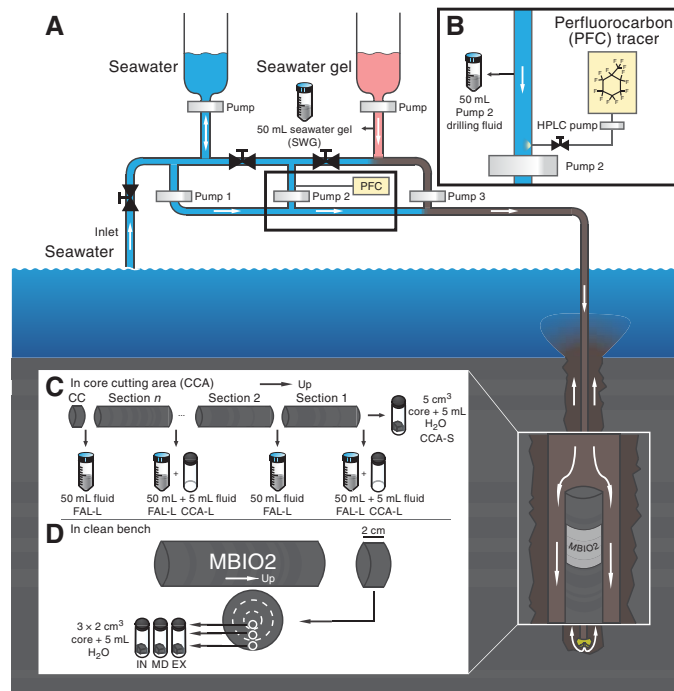
Figure F9. Hydrocarbon gas concentrations, Hole C0023A. Data are from headspace samples taken from dedicated COMGAS WRC slices (sample code 370HS).  $\text{C}_1$  from headspace analyses of safety gas samples taken in core cutting area immediately after arrival on catwalk (sample code HS) is also shown.



Ltd., Japan) was installed in anaerobic chambers located both on the *Chikyu* and at KCC and a clean bench on the *Chikyu*. At KCC, all of the analytical work for microbiology was done in a super-clean room. Ionizers were also installed inside the anaerobic chamber on the *Chikyu* and all sample handling environments at KCC to avoid particle contamination by neutralizing static electricity. The number of airborne particles (0.3–1.0  $\mu\text{m}$  in particle size) in the air of the shipboard working environment was routinely monitored and confirmed to be not detected (ND; <353 particles/m<sup>3</sup>) to  $2.2 \times 10^4$  particles/m<sup>3</sup> in the clean bench and ND to  $1.8 \times 10^5$  particles/m<sup>3</sup> in the anaerobic glove box, whereas the laboratory air on the *Chikyu* contained  $1.12 \times 10^7 \pm 9.46 \times 10^6$  particles/m<sup>3</sup> (mean  $\pm$  SD). At KCC, the vicinity of the work area of the super-clean room was consistently below the detection limit of the particle counter (ND; <117 particles/m<sup>3</sup>). In the anaerobic chamber with a KOACH air filtration system, counts for particles with a diameter of 0.3–2.5  $\mu\text{m}$  ranged from no particles detected (<353 particles/m<sup>3</sup>) prior to sample processing to a maximum of  $10^4$  to  $10^5$  particles/m<sup>3</sup> within 5 min after sample processing.

During Expedition 370, numerous WRC sections and individual samples were collected for microbiological and molecular biological analyses. WRCs for expedition analyses and various postexpedition analyses (e.g., cultivation, activity measurements, and environmental genomics) were initially processed in a clean anaerobic chamber on the *Chikyu* to remove the exteriors of core samples, which came into contact with drilling fluid. After transferring microbiological WRCs to KCC, the sample exterior was further scraped prior to subsampling. This two-step cleaning procedure was important to avoid possible secondary contamination that might occur during

Figure F10. Schematic overview of drilling fluid pumping and contamination sampling procedure used during Expedition 370. A. Pumping of drilling fluid. B. Injection of PFC tracer into drilling fluid. HPLC = high-pressure liquid chromatography. Sampling scheme for (C) drilling fluid contamination test and (D) MBIO2 WRCs (used for DNA analysis). CC = core catcher. L = liquid, S = scraping, FAL = Falcon tube. IN = interior, MD = middle, EX = exterior.



sample processing and improve the level of QC for subsequent microbiological analyses.

To assess the potential of drilling fluid intrusion into the core samples during RCB coring and sample processing, perfluorocarbon (PFC) tracer was added to the drilling fluid stream (Figure F10). The presence of the PFC tracer was tracked within cores and core liner fluid. PFC tracer monitoring during the expedition indicated that the majority of core interiors contained little to undetectable drilling fluid contamination (i.e., for 51 of 117 RCB cores, the interior PFC concentrations were less than the detection limit). Samples of drilling fluid and drilling fluid components (i.e., seawater, gel, etc.) were stored for cell and virus enumeration as well as post-expedition identification of contaminants by molecular biological analysis. The potential of drilling fluid contamination will be carefully assessed by multiple QAs of contamination tracing.

Preliminary results of cell detection and enumeration showed that microbial cell concentrations were distinctly lower than those observed at Site 1174 but at the same time suggested that intact microbial cells are present in low abundance to at least 850 mbst, at which the estimated temperature is approximately 90°C (Figure F11). The complete cell count profile to the sediment/basement interface will be published after ongoing cell enumeration and its validation of data quality. In addition, Expedition 370 provided, for the first time, morphological views of deep subseafloor microbial cells in a low-biomass sediment sample using transmission electron microscopy at KCC (Figure F12). Taxonomic compositions of microbial communities were also analyzed by sequencing PCR-amplified 16S rRNA genes using a MiSeq platform at KCC. The preliminary data showed that, even with such an intensive effort to avoid con-

Figure F11. Preliminary cell count data obtained during Expedition 370, Hole C0023A. Cell counts will be reevaluated postexpedition in light of QC assessments and uncertainty analysis. BD = below detection (dashed line).

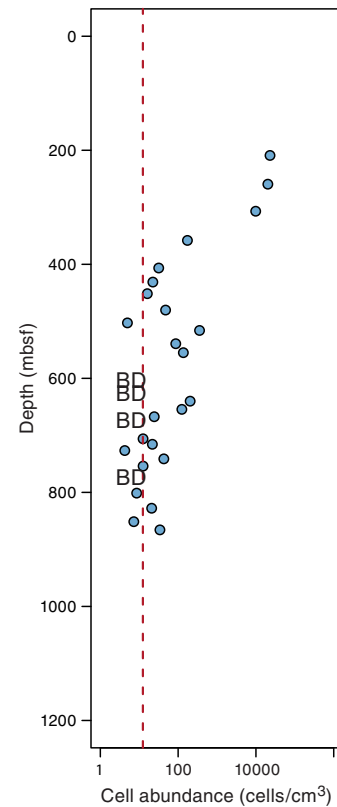
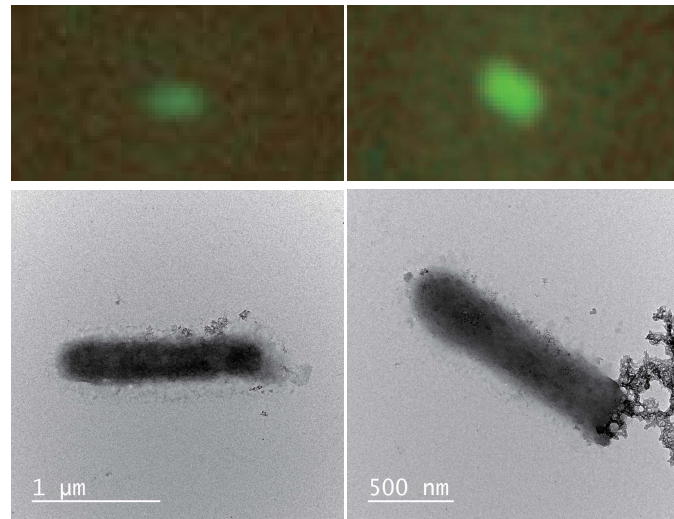


Figure F12. Transmission electron micrographs of microorganisms separated and sorted from sediment (C0023A-6F-2; 304 mbsf).



tamination, it appears not to be free of signals from potential experimental contaminants; this means that more careful efforts on additional molecular analyses (e.g., at single cell to community levels in comparison to data from multiple control samples) will be necessary for low-biomass samples at Site C0023.

To more fully address some of the primary scientific objectives, incubation experiments of fresh sediment samples for potential microbial activity using stable isotope tracers and high-pressure/temperature incubation systems were initiated at KCC. In addition, various types of microbiological and biogeochemical samples were prepared for postexpedition studies, which include samples that will be used for molecular (DNA/RNA and lipid) analyses, activity analyses using radioactive tracers, stable isotope probing combined with secondary-ion mass spectrometry analysis, quantitative functional gene surveys, bioreactor cultivation experiments, probing protein synthesis activity, population of spore-forming microorganism determinations, exoenzyme activity measurements, and virus count and its metagenomic analysis.

## Accomplishments and future prospectus

During Expedition 370, our major operational objectives (cf. Hinrichs et al., 2016) were successfully accomplished through shipboard (*Chikyu*) and onshore (KCC) activities. A large multidisciplinary team was organized for Expedition 370, including biologists, chemists, and geologists, to meet the scientific goals using the latest knowledge and state-of-the-art analytical technologies. As a result, a total of 112 cores were successfully retrieved by the *Chikyu* from Hole C0023A to the sediment/basement interface at 1180 mbsf as originally planned, which is the highest number of cores retrieved by the *Chikyu* from a single borehole so far and covers almost all temperature ranges of life up to ~120°C. All cored samples were processed through X-ray CT image scanning immediately after recovery, and rigorous QA/QC efforts for microbiological and geochemical samples were conducted, using both shipboard and shore-based super-clean facilities for the first time. The high-quality samples obtained during Expedition 370 will be used for various post-expedition research projects, providing an unprecedented opportunity to fully address important and challenging scientific

questions regarding the limits of subseafloor life and the biosphere. Intensive geochemical measurements using high-quality WRC sections as well as geological, sedimentological, and physical property measurements were conducted on board throughout the cored samples at Site C0023. This multidisciplinary data set is crucial because it provides information on environmental conditions that may constrain habitability of subseafloor life and the deep subseafloor biosphere.

After coring operations, we successfully installed thermistor sensor strings into the cased borehole to 863 mbsf. A total of 13 thermistor sensors deployed on a 4 inch tube will monitor temperature above, within, and below the décollement zone, providing a long-term record of borehole temperature equivalent to *in situ* formation. We think that our plan and achievements for the temperature observatory at this particular location are still preliminary and incomplete; a new implementation of long-term observatory systems, including more sensors and *in situ* experimental devices for not only geophysics but also geochemistry and microbiology, would provide another major opportunity for addressing multiple scientific themes and challenges listed in the IODP Science Plan (e.g., biosphere frontiers, Earth connections, and geohazards).

Conclusively, Expedition 370 has, overall, been successful and provided an excellent opportunity to tackle important scientific questions regarding the limits of life in the deep subseafloor biosphere. The expedition, including shipboard and shore-based activities, was completed on 23 November 2016, but our scientific mission to the temperature limit of the deep subseafloor biosphere has just started and will continue over the years at shore-based laboratories with high-quality samples and data retrieved from Site C0023.

## References

Ando, M., 1975. Source mechanisms and tectonic significance of historical earthquakes along the Nankai Trough, Japan. *Tectonophysics*, 27(2):119–140. [http://dx.doi.org/10.1016/0040-1951\(75\)90102-X](http://dx.doi.org/10.1016/0040-1951(75)90102-X)

Aoki, Y., Tamano, T., and Kato, S., 1982. Detailed structure of the Nankai Trough from migrated seismic sections. In Watkins, J.S., and Drake, C.L. (Eds.), *Studies in Continental Margin Geology*. AAPG Memoir, 34:309–322. <http://archives.datapages.com/data/specpubs/history2/data/a110/a110/0001/0300/0309.htm>

Ashi, J., and Taira, A., 1992. Structure of the Nankai accretionary prism as revealed from IZANAGI sidescan imagery and multichannel seismic reflection profiling. *Island Arc*, 1:104–115. <http://dx.doi.org/10.1111/j.1440-1738.1992.tb00063.x>

Bangs, N.L., Shipley, T.H., Gulick, S.P.S., Moore, G.F., Kuromoto, S., and Nakamura, Y., 2004. Evolution of the Nankai Trough décollement from the trench into the seismogenic zone: inferences from three-dimensional seismic reflection imaging. *Geology*, 32(4):273–276. <http://dx.doi.org/10.1130/G20211.2>

Bangs, N.L., Taira, A., Kuramoto, S., Shipley, T.H., Moore, G.F., Mochizuki, K., Gulick, S.S., Zhao, Z., Nakamura, Y., Park, J.-O., Taylor, B.L., Morita, S., Ito, S., Hills, D.J., Leslie, S.C., Alex, C.M., McCutcheon, A.J., Ike, T., Yagi, H., and Toyama, G., 1999. U.S.–Japan collaborative 3-D seismic investigation of the Nankai Trough plate-boundary interface and shallowmost seismogenic zone. *Eos, Transactions of the American Geophysical Union*, 80:569.

Bangs, N.L.B., and Gulick, S.P.S., 2005. Physical properties along the developing décollement in the Nankai Trough: inferences from 3-D seismic reflection data inversion and Leg 190 and 196 drilling data. In Mikada, H., Moore, G.F., Taira, A., Becker, K., Moore, J.C., and Klaus, A. (Eds.), *Proceedings of the Ocean Drilling Program, Scientific Results*, 190/196: College Station, TX (Ocean Drilling Program), 1–18. <http://dx.doi.org/10.2973/odp.proc.sr.190196.354.2005>

Behrmann, J.H., 1991. Conditions for hydrofracture and the fluid permeability of accretionary wedges. *Earth and Planetary Science Letters*, 107(3–4):550–558. [http://dx.doi.org/10.1016/0012-821X\(91\)90100-V](http://dx.doi.org/10.1016/0012-821X(91)90100-V)

Berner, U., and Faber, E., 1993. Light hydrocarbons in sediments of the Nankai accretionary prism (Leg 131, Site 808). In Hill, I.A., Taira, A., Firth, J.V., et al., *Proceedings of the Ocean Drilling Program, Scientific Results*, 131: College Station, TX (Ocean Drilling Program), 185–195. <http://dx.doi.org/10.2973/odp.proc.sr.131.120.1993>

Bethke, C.M., Sanford, R.A., Kirk, M.F., Jin, Q., and Flynn, T.M., 2011. The thermodynamic ladder in geomicrobiology. *American Journal of Science*, 311(3):183–210. <https://doi.org/10.2475/03.2011.01>

Biddle, J.F., Fitz-Gibbon, S., Schuster, S.C., Brenchley, J.E., and House, C.H., 2008. Metagenomic signatures of the Peru margin subseafloor biosphere show a genetically distinct environment. *Proceedings of the National Academy of Sciences of the United States of America*, 105(30):10583–10588. <http://dx.doi.org/10.1073/pnas.0709942105>

Biddle, J.F., Lipp, J.S., Lever, M.A., Lloyd, K.G., Sørensen, K.B., Anderson, R., Fredricks, H.F., Elvert, M., Kelly, T.J., Schrag, D.P., Sogin, M.L., Brenchley, J.E., Teske, A., House, C.H., and Hinrichs, K.-U., 2006. Heterotrophic Archaea dominate sedimentary subsurface ecosystems off Peru. *Proceedings of the National Academy of Sciences of the United States of America*, 103(10):3846–3851. <http://dx.doi.org/10.1073/pnas.0600035103>

Blöchl, E., Rachel, R., Burggraf, S., Hafenbrädl, D., Jannasch, H.W., and Stetter, K.O., 1997. *Pyrolobus fumarii*, gen. and sp. nov., represents a novel group of archaea, extending the upper temperature limit for life to 113°C. *Extremophiles*, 1(1):14–21. <http://www.ncbi.nlm.nih.gov/pubmed/9680332>

Byerlee, J.D., and Summers, R., 1975. Stable sliding preceding stick-slip on fault surfaces in granite at high pressure. *Pure and Applied Geophysics*, 113(1):63–68. <http://dx.doi.org/10.1007/BF01592899>

Chester, F.M., Evans, J.P., and Biegel, R.L., 1993. Internal structure and weakening mechanisms of the San Andreas Fault. *Journal of Geophysical Research: Solid Earth*, 98(B1):771–786. <http://dx.doi.org/10.1029/92JB01866>

Ciobanu, M.-C., Burgaud, G., Dufresne, A., Breuker, A., Rédu, V., Ben Maamar, S., Gaboyer, F., Vandenabeele-Trambouze, O., Lipp, J.S., Schippers, A., Vandenkorrenhuyse, P., Barbier, G., Jebbar, M., Godfroy, A., and Alain, K., 2014. Microorganisms persist at record depths in the subseafloor of the Canterbury Basin. *ISME Journal*, 8:1370–1380. <http://dx.doi.org/10.1038/ismej.2013.250>

Costa Pisani, P., Reshef, M., and Moore, G., 2005. Targeted 3-D prestack depth imaging at Legs 190–196 ODP drill sites (Nankai Trough, Japan). *Geophysical Research Letters*, 32(20):L20309. <http://dx.doi.org/10.1029/2005GL024191>

Coulbourn, W.T., 1986. Explanatory notes. In Kagami, H., Karig, D.E., Coulbourn, W.T., et al., *Initial Reports of the Deep Sea Drilling Project*, 87: Washington, DC (U.S. Government Printing Office). <http://dx.doi.org/10.2973/dsdp.proc.87.102.1986>

D'Hondt, S., Inagaki, F., Alvarez Zarikian, C., Abrams, L.J., Dubois, N., Engelhardt, T., Evans, H., Ferdelman, T., Gribsholt, B., Harris, R.N., Hoppie, B.W., Hyun, J.-H., Kallmeyer, J., Kim, J., Lynch, J.E., McKinley, C.C., Mitsunobu, S., Morono, Y., Murray, R.W., Pockalny, R., Sauvage, J., Shimono, T., Shirashi, F., Smith, D.C., Smith-Duque, C.E., Spivack, A.J., Steinsbu, B.O., Suzuki, Y., Szpak, M., Toffin, L., Uramoto, G., Yamaguchi, Y.T., Zhang, G., Zhang, X.-H., and Ziebis, W., 2015. Presence of oxygen and aerobic communities from sea floor to basement in deep-sea sediments. *Nature Geoscience*, 8(4):299–304. <http://dx.doi.org/10.1038/ngeo2387>

D'Hondt, S., Inagaki, F., Alvarez Zarikian, C.A., and the Expedition 329 Scientists, 2011. *Proceedings of the Integrated Ocean Drilling Program*, 329: Tokyo (Integrated Ocean Drilling Program Management International, Inc.). <http://dx.doi.org/10.2204/iodp.proc.329.2011>

D'Hondt, S., Jørgensen, B.B., Miller, D.J., Batzke, A., Blake, R., Cragg, B.A., Cypionka, H., Dickens, G.R., Ferdelman, T., Hinrichs, K.-U., Holm, N.G., Mitterer, R., Spivack, A., Wang, G., Bekins, B., Engelen, B., Ford, K., Gettemy, G., Rutherford, S.D., Sass, H., Skilbeck, C.G., Aiello, I.W., Guerin, G., House, C.H., Inagaki, F., Meister, P., Naehr, T., Niitsuma, S., Parkes, R.J., Schippers, A., Smith, D.C., Teske, A., Wiegel, J., Naranjo, Padillo, C., and Solis Acosta, J.L., 2004. Distributions of microbial activities in deep subseafloor sediments. *Science*, 306(5705):2216–2221. <http://dx.doi.org/10.1126/science.1101155>

D'Hondt, S., Rutherford, S., and Spivack, A.J., 2002. Metabolic activity of sub-surface life in deep-sea sediments. *Science*, 295(5562):2067–2070. <http://dx.doi.org/10.1126/science.1064878>

D'Hondt, S., Spivack, A.J., Pockalny, R., Ferdelman, T.G., Fischer, J.P., Kallmeyer, J., Abrams, L.J., Smith, D.C., Graham, D., Hasiuk, F., Schrum, H., and Stancine, A.M., 2009. Subseafloor sedimentary life in the South Pacific Gyre. *Proceedings of the National Academy of Sciences of the United States of America*, 106(28):11651–11656. <http://dx.doi.org/10.1073/pnas.0811793106>

Glombitsa, C., Adhikari, R.R., Riedinger, N., Gilhooly, W.P., III, Hinrichs, K.-U., and Inagaki, F., 2016. Microbial sulfate reduction potential in coal-bearing sediments down to ~2.5 km below the seafloor off Shimokita Peninsula, Japan. *Frontiers in Microbiology*, 7:1576. <https://doi.org/10.3389/fmicb.2016.01576>

Gulick, S.P.S., Bangs, N.L.B., Shipley, T.H., Nakamura, Y., Moore, G., and Kuramoto, S., 2004. Three-dimensional architecture of the Nankai accretionary prism's imbricate thrust zone off Cape Muroto, Japan: prism reconstruction via en echelon thrust propagation. *Journal of Geophysical Research: Solid Earth*, 109(B2):B02105. <http://dx.doi.org/10.1029/2003JB002654>

Harris, R., Yamano, M., Kinoshita, M., Spinelli, G., Hamamoto, H., and Ashi, J., 2013. A synthesis of heat flow determinations and thermal modeling along the Nankai Trough, Japan. *Journal of Geophysical Research: Solid Earth*, 118(6):2687–2702. <http://dx.doi.org/10.1002/jgrb.50230>

Head, I.M., Jones, D.M., and Larter, S.R., 2003. Biological activity in the deep subsurface and the origin of heavy oil. *Nature*, 426(6964):344–352. <http://dx.doi.org/10.1038/nature02134>

Heberling, C., Lowell, R.P., Liu, L., and Fisk, M.R., 2010. Extent of the microbial biosphere in the oceanic crust. *Geochemistry, Geophysics, Geosystems*, 11(8):Q08003. <http://dx.doi.org/10.1029/2009GC002968>

Heuer, V., Elvert, M., Tille, S., Krummen, M., Prieto Mollar, X., Hmelo, L.R., and Hinrichs, K.-U., 2006. Online  $\delta^{13}\text{C}$  analysis of volatile fatty acids in sediment/porewater systems by liquid chromatography-isotope ratio mass spectrometry. *Limnology and Oceanography: Methods*, 4:346–357. <http://dx.doi.org/10.4319/lom.2006.4.346>

Heuer, V.B., Pohlman, J.W., Torres, M.E., Elvert, M., and Hinrichs, K.-U., 2009. The stable carbon isotope biogeochemistry of acetate and other dissolved carbon species in deep subseafloor sediments at the northern Cascadia margin. *Geochimica et Cosmochimica Acta*, 73(11):3323–3336. <http://dx.doi.org/10.1016/j.gca.2009.03.001>

Hinrichs, K.-U., and Inagaki, F., 2012. Downsizing the deep biosphere. *Science*, 338(6104):204–205. <http://dx.doi.org/10.1126/science.1229296>

Hinrichs, K.-U., Inagaki, F., Heuer, V.B., Kinoshita, M., Morono, Y., and Kubo, Y., 2016. *Expedition 370 Scientific Prospectus: T-Limit of the Deep Biosphere off Muroto (T-Limit)*. International Ocean Discovery Program. <http://dx.doi.org/10.14379/iodp.sp.370.2016>

Hoehler, T.M., 2004. Biological energy requirements as quantitative boundary conditions for life in the subsurface. *Geobiology*, 2(4):205–215. <https://doi.org/10.1111/j.1472-4677.2004.00033.x>

Hoehler, T.M., and Jørgensen, B.B., 2013. Microbial life under extreme energy limitation. *National Review of Microbiology*, 11(2):83–94. <https://doi.org/10.1038/nrmicro2939>

Horsfield, B., Schenk, H.J., Zink, K., Ondrák, R., Dieckmann, V., Kallmeyer, J., Mangelsdorf, K., di Primio, R., Wilkes, H., Parkes, R.J., Fry, J., and Cragg, B., 2006. Living microbial ecosystems within the active zone of catagenesis: implications for feeding the deep biosphere. *Earth and Planetary Science Letters*, 246(1–2):55–69. <http://dx.doi.org/10.1016/j.epsl.2006.03.040>

Hüpers, A., and Kopf, A.J., 2009. The thermal influence on the consolidation state of underthrust sediments from the Nankai margin and its implications for excess pore pressure. *Earth and Planetary Science Letters*, 286(1–2):324–332. <http://dx.doi.org/10.1016/j.epsl.2009.05.047>

Ikari, M.J., Saffer, D.M., and Marone, C., 2009. Frictional and hydrologic properties of a major splay fault system, Nankai subduction zone. *Geophysical*

Research Letters, 36(20):L20313.  
<http://dx.doi.org/10.1029/2009GL040009>

Imachi, H., Aoi, K., Tasumi, E., Saito, Y., Yamanaka, Y., Saito, Y., Yamaguchi, T., Tomaru, H., Takeuchi, R., Morono, Y., Inagaki, F., and Takai, K., 2011. Cultivation of methanogenic community from subseafloor sediments using a continuous-flow bioreactor. *ISME Journal*, 5(12):1751–1925.  
<https://doi.org/10.1038/ismej.2011.64>

Inagaki, F., Hinrichs, K.-U., Kubo, Y., Bowles, M.W., Heuer, V.B., Long, W.-L., Hoshino, T., Ijiri, A., Imachi, H., Ito, M., Kaneko, M., Lever, M.A., Lin, Y.-S., Methé, B.A., Morita, S., Morono, Y., Tanikawa, W., Bihan, M., Bowden, S.A., Elvert, M., Glombitza, C., Gross, D., Harrington, G.J., Hori, T., Li, K., Limmer, D., Liu, C.-H., Murayama, M., Ohkouchi, N., Ono, S., Park, Y.-S., Phillips, S.C., Prieto-Mollar, X., Purkey, M., Riedinger, N., Sanada, Y., Sauvage, J., Snyder, G., Susilawati, R., Takano, Y., Tasumi, E., Terada, T., Tomaru, H., Trembath-Reichert, E., Wang, D.T., and Yamada, Y., 2015. Exploring deep microbial life in coal-bearing sediment down to ~2.5 km below the ocean floor. *Science*, 349(6246):420–424.  
<http://dx.doi.org/10.1126/science.aaa6882>

Inagaki, F., Nunoura, T., Nakagawa, S., Teske, A., Lever, M., Lauer, A., Suzuki, M., Takai, K., Delwiche, M., Colwell, F.S., Nealson, K.H., Horikoshi, K., D'Hondt, S., and Jørgensen, B.B., 2006. Biogeographical distribution and diversity of microbes in methane hydrate-bearing deep marine sediments on the Pacific Ocean margin. *Proceedings of the National Academy of Sciences of the United States of America*, 103(8):2815–2820.  
<http://dx.doi.org/10.1073/pnas.0511033103>

Kallmeyer, J., 2011. Detection and quantification of microbial cells in subsurface sediments. *Advances in Applied Microbiology*, 76:79–103.  
<http://dx.doi.org/10.1016/B978-0-12-387048-3.00003-9>

Kallmeyer, J., Pockalny, R., Adhikari, R.R., Smith, D.C., and D'Hondt, S., 2012. Global distribution of microbial abundance and biomass in subseafloor sediment. *Proceedings of the National Academy of Sciences of the United States of America*, 109(40):16213–16216.  
<http://dx.doi.org/10.1073/pnas.1203849109>

Karig, D.E., 1986. The framework of deformation in the Nankai Trough. In Kagami, N., Karig, D.E., Coulbourn, W.T., et al., *Initial Reports of the Deep Sea Drilling Project*, 87: Washington, DC (U.S. Government Printing Office), 927–940. <http://dx.doi.org/10.2973/dsdp.proc.87.138.1986>

Kashefi, K., and Lovley, D.R., 2003. Extending the upper temperature limit for life. *Science*, 301(5635):934. <http://dx.doi.org/10.1126/science.1086823>

Kastner, M., Elderfield, H., Jenkins, W.J., Gieskes, J.M., and Gamo, T., 1993. Geochemical and isotopic evidence for fluid flow in the western Nankai subduction zone, Japan. In Hill, I.A., Taira, A., Firth, J.V., et al., *Proceedings of the Ocean Drilling Program, Scientific Results*, 131: College Station, TX (Ocean Drilling Program), 397–413.  
<http://dx.doi.org/10.2973/odp.proc.sr.131.143.1993>

Kinoshita, H., and Yamano, M., 1986. The heat flow anomaly in the Nankai Trough area. In Kagami, H., Karig, D.E., Coulbourn, W.T., et al., *Initial Reports of the Deep Sea Drilling Project*, 87: Washington, DC (U.S. Government Printing Office), 737–743.  
<http://dx.doi.org/10.2973/dsdp.proc.87.121.1986>

Kodaira, S., Takahashi, N., Park, J.-O., Mochizuki, K., Shinohara, M., and Kimura, S., 2000. Western Nankai Trough seismogenic zone: results from a wide-angle ocean bottom seismic survey. *Journal of Geophysical Research: Solid Earth*, 105(B3):5887–5905.  
<http://dx.doi.org/10.1029/1999JB900394>

Langerhuus, A.T., Røy, H., Lever, M.A., Morono, Y., Inagaki, F., Jørgensen, B.B., and Lomstein, B.A., 2012. Endospore abundance and D:L-amino acid modeling of bacterial turnover in Holocene marine sediment (Aarhus Bay). *Geochimica et Cosmochimica Acta*, 99:87–99.  
<https://doi.org/10.1016/j.gca.2012.09.023>

Le Pichon, X., Iiyama, T., Chamley, H., Charvet, J., Faure, M., Fujimoto, H., Furuta, T., Ida, Y., Kagami, H., Lallemand, S., Leggett, J., Murata, A., Okada, H., Rangin, C., Renard, V., Taira, A., and Tokuyama, H., 1987. Nankai Trough and the fossil Shikoku Ridge: results of Box 6 *Kaiko* survey. *Earth and Planetary Science Letters*, 83(1–4):186–198.  
[http://dx.doi.org/10.1016/0012-821X\(87\)90065-3](http://dx.doi.org/10.1016/0012-821X(87)90065-3)

Lever, M.A., Rouxel, O., Alt, J.C., Shimizu, N., Ono, S., Coggan, R.M., Shanks, W.C., III, Laphan, L., Elvert, M., Prieto-Mollar, X., Hinrichs, K.-U., Inagaki, F., and Teske, A., 2013. Evidence for microbial carbon and sulfur cycling in deeply buried ridge flank basalt. *Science*, 339(6125):1305–1308.  
<http://dx.doi.org/10.1126/science.1229240>

Lever, M.A., Torti, A., Eickenbusch, P., Michaud, A.B., Šantl-Temkiv, T., and Jørgensen, B.B., 2015. A modular method for the extraction of DNA and RNA, and the separation of DNA pools from diverse environmental sample types. *Frontiers in Microbiology*, 6:1–25.  
<http://dx.doi.org/10.3389/fmicb.2015.00476>

Lipp, J.S., Morono, Y., Inagaki, F., and Hinrichs, K.-U., 2008. Significant contribution of Archaea to extant biomass in marine subsurface sediments. *Nature*, 454(7207):991–994. <http://dx.doi.org/10.1038/nature07174>

Liu, C.-H., Huang, X., Xie, T.-N., Duan, N., Xue, Y.-R., Zhao, T.-X., Lever, M.A., Hinrichs, K.-U., and Inagaki, F., 2017. Exploration of cultivable fungal communities in deep coal-bearing sediments from ~1.3 to 2.5 km below the ocean floor. *Environmental Microbiology*, 19(2):803–818.  
<https://doi.org/10.1111/1462-2920.13653>

Lloyd, K.G., Schreiber, L., Petersen, D.G., Kjeldsen, K.U., Lever, M.A., Steen, A.D., Stepanauskas, R., Richter, M., Kleindienst, S., Lenk, S., Schramm, A., and Jørgensen, B.B., 2013. Predominant Archaea in marine sediments degrade detrital proteins. *Nature*, 496(7444):215–218.  
<http://dx.doi.org/10.1038/nature12033>

Lomstein, B.A., Langerhuus, A.T., D'Hondt, S., Jørgensen, B.B., and Spivack, A., 2012. Endospore abundance, microbial growth and necromass turnover in deep sub-seafloor sediment. *Nature*, 484(7392):101–104.  
<http://dx.doi.org/10.1038/nature10905>

Mair, K., and Marone, C., 1999. Friction of simulated fault gouge for a wide range of velocities and normal stresses. *Journal of Geophysical Research: Solid Earth*, 104(B12):28899–28914.  
<http://dx.doi.org/10.1029/1999JB900279>

Maltman, A., Byrne, T., Karig, D., Lallement, S., and the Leg 131 Shipboard Party, 1992. Structural geological evidence from ODP Leg 131 regarding fluid flow in the Nankai prism, Japan. *Earth and Planetary Science Letters*, 109(3–4):463–468. [http://dx.doi.org/10.1016/0012-821X\(92\)90106-6](http://dx.doi.org/10.1016/0012-821X(92)90106-6)

Mikada, H., Becker, K., Moore, J.C., Klaus, A., et al., 2002. *Proceedings of the Ocean Drilling Program, Initial Reports*, 196: College Station, TX (Ocean Drilling Program). <http://dx.doi.org/10.2973/odp.proc.ir.196.2002>

Moore, G.E., Karig, D.E., Shipley, T.H., Taira, A., Stoffa, P.L., and Wood, W.T., 1991. Structural framework of the ODP Leg 131 area, Nankai Trough. In Taira, A., Hill, I., Firth, J.V., et al., *Proceedings of the Ocean Drilling Program, Initial Reports*, 131: College Station, TX (Ocean Drilling Program), 15–20. <http://dx.doi.org/10.2973/odp.proc.ir.131.102.1991>

Moore, G.E., Shipley, T.H., Stoffa, P.L., Karig, D.E., Taira, A., Kuramoto, S., Tokuyama, H., and Suyehiro, K., 1990. Structure of the Nankai Trough accretionary zone from multichannel seismic reflection data. *Journal of Geophysical Research: Solid Earth*, 95(B6):8753–8765.  
<http://dx.doi.org/10.1029/JB095iB06p08753>

Moore, G.E., Taira, A., Klaus, A., et al., 2001. *Proceedings of the Ocean Drilling Program, Initial Reports*, 190: College Station, TX (Ocean Drilling Program). <http://dx.doi.org/10.2973/odp.proc.ir.190.2001>

Moore, J.C., and Saffer, D., 2001. Updip limit of the seismogenic zone beneath the accretionary prism of southwest Japan: an effect of diagenetic to low-grade metamorphic processes and increasing effective stress. *Geology*, 29(2):183–186. [http://dx.doi.org/10.1130/0091-7613\(2001\)029<0183:ULOTSZ>2.0.CO;2](http://dx.doi.org/10.1130/0091-7613(2001)029<0183:ULOTSZ>2.0.CO;2)

Morono, Y., and Inagaki, F., 2010. Automatic slide-loader fluorescent microscope for discriminative enumeration of subseafloor life. *Scientific Drilling*, 9:32–36. <http://dx.doi.org/10.2204/iodp.sd.9.06.2010>

Morono, Y., Terada, T., Hoshino, T., Inagaki, F., and Kostka, J.E. (Ed.), 2014. Hot-alkaline DNA extraction method for deep-subseafloor archaeal communities. *Applied and Environmental Microbiology*, 80(6):1985–1994.  
<http://dx.doi.org/10.1128/AEM.04150-13>

Morono, Y., Terada, T., Kallmeyer, J., and Inagaki, F., 2013. An improved cell separation technique for marine subsurface sediments: applications for high-throughput analysis using flow cytometry and cell sorting. *Environ-*

*mental Microbiology*, 15(10):2841–2849.  
<http://dx.doi.org/10.1111/1462-2920.12153>

Morono, Y., Terada, T., Masui, N., and Inagaki, F., 2009. Discriminative detection and enumeration of microbial life in marine subsurface sediments. *The ISME Journal*, 3(5):503–511.  
<http://dx.doi.org/10.1038/ismej.2009.1>

Morono, Y., Terada, T., Nishizawa, M., Ito, M., Hillion, F., Takahata, N., Sano, Y., and Inagaki, F., 2011. Carbon and nitrogen assimilation in deep seafloor microbial cells. *Proceedings of the National Academy of Sciences of the United States of America*, 108(45):18295–18300.  
<http://dx.doi.org/10.1073/pnas.1107763108>

Okino, K., and Kato, Y., 1995. Geomorphological study on a clastic accretionary prism: the Nankai Trough. *Island Arc*, 4(3):182–198.  
<http://dx.doi.org/10.1111/j.1440-1738.1995.tb00142.x>

Orcutt, B.N., Bach, W., Becker, K., Fisher, A.T., Hentscher, M., Toner, B.M., Wheat, C.G., and Edwards, K.J., 2011. Colonization of subsurface microbial observatories deployed in young ocean crust. *ISME Journal*, 5(4):692–703. <http://dx.doi.org/10.1038/ismej.2010.157>

Orsi, W.D., Edgcomb, V.P., Christman, G.D., and Biddle, J.F., 2013. Gene expression in the deep biosphere. *Nature*, 499(7457):205–208.  
<http://dx.doi.org/10.1038/nature12230>

Park, J.-O., Tsuru, T., Kaneda, Y., Kono, Y., Kodaira, S., Takahashi, N., and Kinoshita, H., 1999. A subducting seamount beneath the Nankai accretionary prism off Shikoku, southwestern Japan. *Geophysical Research Letters*, 26(7):931–934. <http://dx.doi.org/10.1029/1999GL900134>

Park, J.-O., Tsuru, T., Kodaira, S., Nakanishi, A., Miura, S., Kaneda, Y., Kono, Y., and Takahashi, N., 2000. Out-of-sequence thrust faults developed in the coseismic slip zone of the 1946 Nankai earthquake (Mw = 8.2) off Shikoku, southwest Japan. *Geophysical Research Letters*, 27(7):1033–1036. <http://dx.doi.org/10.1029/1999GL008443>

Parkes, R.J., Cragg, B., Roussel, E., Webster, G., Weightman, A., and Sass, H., 2014. A review of prokaryotic populations and processes in sub-seafloor sediments, including biosphere:geosphere interactions. *Marine Geology*, 352:409–425. <http://dx.doi.org/10.1016/j.margeo.2014.02.009>

Parkes, R.J., Cragg, B.A., Bale, S.J., Getliff, J.M., Goodman, K., Rochelle, P.A., Fry, J.C., Weightman, A.J., and Harvey, S.M., 1994. Deep bacterial biosphere in Pacific Ocean sediments. *Nature*, 371(6496):410–413.  
<http://dx.doi.org/10.1038/371410a0>

Parkes, R.J., Cragg, B.A., and Wellsbury, P., 2000. Recent studies on bacterial populations and processes in subseafloor sediments: a review. *Hydrogeology Journal*, 8(1):11–28. <http://dx.doi.org/10.1007/PL00010971>

Parkes, R.J., Wellsbury, P., Mather, I.D., Cobb, S.J., Cragg, B.A., Hornibrook, E.R.C., and Horsfield, B., 2007. Temperature activation of organic matter and minerals during burial has the potential to sustain the deep biosphere over geological timescales. *Organic Geochemistry*, 38(6):845–852.  
<http://dx.doi.org/10.1016/j.orggeochem.2006.12.011>

Roussel, E.G., Cambon Bonavita, M.-A., Querellou, J., Cragg, B.A., Webster, G., Prieur, D., and Parkes, J.R., 2008. Extending the sub-sea-floor biosphere. *Science*, 320(5879):1046.  
<http://dx.doi.org/10.1126/science.1154545>

Roussel, E.G., Cragg, B.A., Webster, G., Sass, H., Tang, X., Williams, A.S., Gorra, R., Weightman, A.J., and Parkes, R.J., 2015. Complex coupled metabolic and prokaryotic community responses to increasing temperatures in anaerobic marine sediments: critical temperatures and substrate changes. *FEMS Microbiology Ecology*, 91(8):fiv084.  
<http://dx.doi.org/10.1093/femsec/fiv084>

Røy, H., Kallmeyer, J., Adhikari, R.R., Pockalny, R., Jørgensen, B.B., and D'Hondt, S., 2012. Aerobic microbial respiration in 86-million-year-old deep-sea red clay. *Science*, 336(6083):922–925.  
<http://dx.doi.org/10.1126/science.1219424>

Saffer, D.M., and Bekins, B.A., 1998. Episodic fluid flow in the Nankai accretionary complex: timescale, geochemistry, flow rates, and fluid budget. *Journal of Geophysical Research: Solid Earth*, 103(B12):30351–30371.  
<http://dx.doi.org/10.1029/98JB01983>

Seno, T., Stein, S., and Gripp, A.E., 1993. A model for the motion of the Philippine Sea plate consistent with NUVEL-1 and geological data. *Journal of Geophysical Research: Solid Earth*, 98(B10):17941–17948.  
<http://dx.doi.org/10.1029/93JB00782>

Shipboard Scientific Party, 1975a. Site 290. In Karig, D.E., Ingle, J.C., Jr., et al., *Initial Reports of the Deep Sea Drilling Project*, 31: Washington, DC (U.S. Government Printing Office), 25–47.  
<http://dx.doi.org/10.2973/dsdp.proc.31.102.1975>

Shipboard Scientific Party, 1975b. Site 298. In Karig, D.E., Ingle, J.C., Jr., et al., *Initial Reports of the Deep Sea Drilling Project*, 31: Washington, DC (U.S. Government Printing Office), 317–350.  
<http://dx.doi.org/10.2973/dsdp.proc.31.109.1975>

Shipboard Scientific Party, 1991. Site 808. In Taira, A., Hill, I., Firth, J.V., et al., *Proceedings of the Ocean Drilling Program, Initial Reports*, 131: College Station, TX (Ocean Drilling Program), 71–269.  
<http://dx.doi.org/10.2973/odp.proc.ir.131.106.1991>

Shipboard Scientific Party, 2001a. Leg 190 summary. In Moore, G.F., Taira, A., Klaus, A., et al., *Proceedings of the Ocean Drilling Program, Initial Reports*, 190: College Station, TX (Ocean Drilling Program), 1–87.  
<http://dx.doi.org/10.2973/odp.proc.ir.190.101.2001>

Shipboard Scientific Party, 2001b. Site 1173. In Moore, G.F., Taira, A., Klaus, A., et al., *Proceedings of the Ocean Drilling Program, Initial Reports*, 190: College Station, TX (Ocean Drilling Program), 1–147.  
<http://dx.doi.org/10.2973/odp.proc.ir.190.104.2001>

Shipboard Scientific Party, 2001c. Site 1174. In Moore, G.F., Taira, A., Klaus, A., et al., *Proceedings of the Ocean Drilling Program, Initial Reports*, 190: College Station, TX (Ocean Drilling Program), 1–149.  
<http://dx.doi.org/10.2973/odp.proc.ir.190.105.2001>

Sogin, M.L., Morrison, H.G., Huber, J.A., Welch, D.M., Huse, S.M., Neal, P.R., Arrieta, J.M., and Herndl, G.J., 2006. Microbial diversity in the deep sea and the underexplored “rare biosphere.” *Proceedings of the National Academy of Sciences of the United States of America*, 103(32):12115–12120.  
<http://dx.doi.org/10.1073/pnas.0605127103>

Spinelli, G.A., Mozley, P.S., Tobin, H.J., Underwood, M.B., Hoffman, N.W., and Bellew, G.M., 2007. Diagenesis, sediment strength, and pore collapse in sediment approaching the Nankai Trough subduction zone. *Geological Society of America Bulletin*, 119(3–4):377–390.  
<http://dx.doi.org/10.1130/B25920.1>

Spinelli, G.A., and Underwood, M.B., 2005. Modeling thermal history of subducting crust in Nankai Trough: constraints from in situ sediment temperature and diagenetic reaction progress. *Geophysical Research Letters*, 32(9):L09301. <http://dx.doi.org/10.1029/2005GL022793>

Spinelli, G.A., and Wang, K., 2008. Effects of fluid circulation in subduction crust on Nankai margin seismogenic zone temperatures. *Geology*, 36(11):887–890. <http://dx.doi.org/10.1130/G25145A.1>

Stoffa, P.L., Wood, W.T., Shipley, T.H., Moore, G.F., Nishiyama, E., Bothelo, M.A.B., Taira, A., Tokuyama, H., and Suyehiro, K., 1992. Deepwater high-resolution expanding spread and split spread marine seismic profiles in the Nankai Trough. *Journal of Geophysical Research: Solid Earth*, 97(B2):1687–1713. <http://dx.doi.org/10.1029/91JB02606>

Taira, A., and Ashi, J., 1993. Sedimentary facies evolution of the Nankai forearc and its implications for the growth of the Shimanto accretionary prism. In Hill, I.A., Taira, A., Firth, J.V., et al., *Proceedings of the Ocean Drilling Program, Scientific Results*, 131: College Station, TX (Ocean Drilling Program), 331–341.  
<http://dx.doi.org/10.2973/odp.proc.sr.131.136.1993>

Taira, A., Hill, I., Firth, J., Berner, U., Brückmann, W., Byrne, T., Chabernaud, T., Fisher, A., Foucher, J.-P., Gamo, T., Gieskes, J., Hyndman, R., Karig, D., Kastner, M., Kato, Y., Lallement, S., Lu, R., Maltman, A., Moore, G., Moran, K., Olafsson, G., Owens, W., Pickering, K., Siena, F., Taylor, E., Underwood, M., Wilkinson, C., Yamano, M., and Zhang, J., 1992. Sediment deformation and hydrogeology of the Nankai Trough accretionary prism: synthesis of shipboard results of ODP Leg 131. *Earth and Planetary Science Letters*, 109(3–4):431–450.  
[http://dx.doi.org/10.1016/0012-821X\(92\)90104-4](http://dx.doi.org/10.1016/0012-821X(92)90104-4)

Taira, A., Hill, I., Firth, J.V., et al., 1991. *Proceedings of the Ocean Drilling Program, Initial Reports*, 131: College Station, TX (Ocean Drilling Program).  
<http://dx.doi.org/10.2973/odp.proc.ir.131.1991>

Takai, K., Mottl, M.J., Nielsen, S.H., and the Expedition 331 Scientists, 2011. *Proceedings of the Integrated Ocean Drilling Program*, 331: Tokyo (Integrated Ocean Drilling Program Management International, Inc.). <http://dx.doi.org/10.2204/iodp.proc.331.2011>

Takai, K., Nakamura, K., Toki, T., Tsunogai, U., Miyazaki, M., Miyazaki, J., Hirayama, H., Nakagawa, S., Nunoura, T., and Horikoshi, K., 2008. Cell proliferation at 122°C and isotopically heavy CH<sub>4</sub> production by a hyperthermophilic methanogen under high-pressure cultivation. *Proceedings of the National Academy of Sciences of the United States of America*, 105(31):10949–10954. <http://dx.doi.org/10.1073/pnas.0712334105>

Towe, K.M., 1962. Clay mineral diagenesis as a possible source of silica cement in sedimentary rocks. *Journal of Sedimentary Research*, 32(1):26–28. <http://dx.doi.org/10.1306/74D70C3B-2B21-11D7-8648000102C1865D>

Underwood, M.B., Orr, R., Pickering, K., and Taira, A., 1993. Provenance and dispersal patterns of sediments in the turbidite wedge of Nankai Trough. In Hill, I.A., Taira, A., Firth, J.V., et al., *Proceedings of the Ocean Drilling Program, Scientific Results*, 131: College Station, TX (Ocean Drilling Program), 15–34. <http://dx.doi.org/10.2973/odp.proc.sr.131.105.1993>

Vrolijk, P., 1990. On the mechanical role of smectite in subduction zones. *Geology*, 18(8):703–707. [http://dx.doi.org/10.1130/0091-7613\(1990\)018<0703:OTMROS>2.3.CO;2](http://dx.doi.org/10.1130/0091-7613(1990)018<0703:OTMROS>2.3.CO;2)

Wang, D.T., Gruen, D.S., Sherwood Lollar, B., Hinrichs, K.-U., Stewart, L.C., Holden, J.F., Hristov, A.N., Pohlman, J.W., Morrill, P.L., Könneke, M., Delwiche, K.B., Reeves, E.P., Sutcliffe, C.N., Ritter, D.J., Seewald, J.S., McIntosh, J.C., Hemond, H.F., Kubo, M.D., Cardace, D., Hoehler, T.M., and Ono, S., 2015. Nonequilibrium clumped isotope signals in microbial methane. *Science*, 348(6233):428–431. <http://dx.doi.org/10.1126/science.aaa4326>

Wang, G., Spivack, A.J., and D'Hondt, S., 2010. Gibbs energies of reaction and microbial mutualism in anaerobic deep subseafloor sediments of ODP Site 1226. *Geochimica et Cosmochimica Acta*, 74(14):3938–3947. <https://doi.org/10.1016/j.gca.2010.03.034>

Wegener, G., Bausch, M., Holler, T., Thang, N.M., Prieto Mollar, X., Kellermann, M.Y., Hinrichs, K.-U., and Boetius, A., 2012. Assessing sub-seafloor microbial activity by combined stable isotope probing with deuterated water and <sup>13</sup>C-bicarbonate. *Environmental Microbiology*, 14(6):1517–1527. <http://dx.doi.org/10.1111/j.1462-2920.2012.02739.x>

Whitman, W.B., Coleman, D.C., and Wiebe, W.J., 1998. Prokaryotes: the unseen majority. *Proceedings of the National Academy of Sciences of the United States of America*, 95(12):6578–6583. <http://dx.doi.org/10.1073/pnas.95.12.6578>

Wilhelms, A., Larter, S.R., Head, I., Farrimond, P., di-Primio, R., and Zwach, C., 2001. Biodegradation of oil in uplifted basins prevented by deep-burial sterilization. *Nature*, 411(6841):1034–1037. <http://dx.doi.org/10.1038/35082535>

Wintsch, R.P., Christoffersen, R., and Kronenberg, A.K., 1995. Fluid-rock reaction weakening of fault zones. *Journal of Geophysical Research: Solid Earth*, 100(B7):13021–13032. <http://dx.doi.org/10.1029/94JB02622>

Yamano, M., Foucher, J.-P., Kinoshita, M., Fisher, A., Hyndman, R.D., and ODP Leg 131 Shipboard Scientific Party, 1992. Heat flow and fluid flow regime in the western Nankai accretionary prism. *Earth and Planetary Science Letters*, 109(3–4):451–462. [http://dx.doi.org/10.1016/0012-821X\(92\)90105-5](http://dx.doi.org/10.1016/0012-821X(92)90105-5)

Yamano, M., Honda, S., and Uyeda, S., 1984. Nankai Trough: a hot trench? *Marine Geophysical Researches*, 6(2):187–203. <http://dx.doi.org/10.1007/BF00285959>

Yanagawa, K., Breuker, A., Schippers, A., Nishizawa, M., Ijiri, A., Hirai, M., Takaki, Y., Sunamura, M., Urabe, T., Nunoura, T., and Takai, K., 2014. Microbial community stratification controlled by the subseafloor fluid flow and geothermal gradient at the Iheya North hydrothermal field in the mid-Okinawa Trough (Integrated Ocean Drilling Program Expedition 331). *Applied and Environmental Microbiology*, 80(19):6126–6135. <http://dx.doi.org/10.1128/aem.01741-14>

Yanagawa, K., Ijiri, A., Breuker, A., Sakai, S., Miyoshi, Y., Kawagucci, S., Noguchi, T., Hirai, M., Schippers, A., Ishibashi, J., Takaki, Y., Sunamura, M., Urabe, T., Nunoura, T., and Takai, K., 2016. Defining boundaries for the distribution of microbial communities beneath the sediment-buried, hydrothermally active seafloor. *JSME Journal*, 11(2):529–542. <https://doi.org/10.1038/ismej.2016.119>

Zhuang, G.-H., Lin, Y.-S., Elvert, M., Heuer, V.B., and Hinrichs, K.-U., 2014. Gas chromatographic analysis of methanol and ethanol in marine sediment pore waters: validation and implementation of three pretreatment techniques. *Marine Chemistry*, 160:82–90. <http://dx.doi.org/10.1016/j.marchem.2014.01.011>